

## ABSTRACT

HYDE, GARY KEVIN. Electrostatic Self-assembled Nanolayers on Textile Fibers. (Under the direction of Juan P. Hinestroza.)

This project reports the deposition of nanolayers of poly(sodium 4-styrene sulfonate) (PSS) and poly(allylamine hydrochloride) (PAH) over cotton fibers using the electrostatic self-assembly method (ESA). While glass, silicon wafers, gold coated particles, quartz and mica have dominated the choice of substrates for ESA, the use of textile fibers has been rarely considered. Cotton, in particular, offers a unique challenge to the deposition of nanolayers because of its unique cross section as well as the chemical heterogeneity of its surface.

The deposition of the nanolayers involved the preparation of cotton substrates via immersion in 2,3-epoxypropyltrimethylammonium chloride solutions to produce cotton with a high density of cationic groups. The cationic cotton was processed further by repeated sequential dipping into aqueous solutions of PSS and PAH with rinsing between each deposition step. Attenuated Total Reflectance Fourier Transform Infrared Spectroscopy (FTIR), X-ray Photoelectron Spectroscopy (XPS), and Transmission Electron Microscopy (TEM) were used to verify the presence of deposited nanolayers. This research work demonstrates the possibility of using the ESA method to tailor the surface of textile fibers at the molecular level by depositing nanolayers of biocidal, charged nanoparticles, non-reactive dyes, and polyelectrolytes in a controlled manner. Preliminary results indicate that the thickness and sequence of the nanolayers can be controlled to tailor and enhance the selectivity, diffusivity, and permeability of the textile fibers while maintaining their comfort and physical properties.

**ELECTROSTATIC SELF-ASSEMBLED NANOLAYERS  
ON TEXTILE FIBERS**

by

**GARY KEVIN HYDE**

A thesis submitted to the Graduate Faculty of

North Carolina State University

in partial fulfillment of the

requirements for the Degree of

Master of Science

In

Polymer and Color Chemistry

Raleigh, NC

2005

**APPROVED BY:**



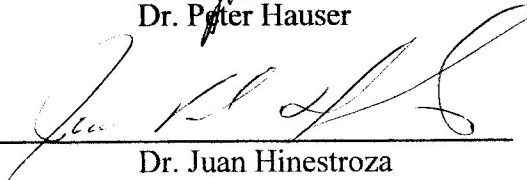
Dr. William Oxenham



Dr. Peter Hauser



Dr. Lei Qian



Dr. Juan Hinstroza  
(Chair of Advisory Committee)

## **DEDICATION**

I would like to dedicate this work to my mom and dad. Thanks for everything.

## **BIOGRAPHY**

Gary Kevin Hyde was born on June 24, 1981 to Gary and Karen Hyde of Ellijay, GA. Kevin has one sister, Amanda. He graduated from Gilmer High School in Ellijay, GA in May 1999. Kevin graduated Magna Cum Laude with a Bachelor of Science degree in Textile Engineering Technology in May 2003 from Southern Polytechnic State University in Marietta, GA. After graduation, Kevin began attending North Carolina State University to pursue a Master's of Science degree in Textile Chemistry as an Institute of Textile Technology Fellow. After completing his master's degree, Kevin hopes to work as an engineer in the textile industry.

## **ACKNOWLEDGMENTS**

I would like to thank Dr. Hineostroza for his guidance, support, and hard work throughout this project. Special thanks to Dr. Mariana Rusa for her time and help preparing samples and analyzing data. Thanks to all of the students who helped prepare some of the samples: Marc Matthews, Jordan Massey, Christina Diaz, and Amika Rokovich. Thank you to Brian Shiels for his help in the lab. I also would like to thank Dr. Mark Walters and the SMIF lab at Duke University for the use of their XPS and TEM systems and all of their help and time.

Thank you to the Institute of Textile Technology for their financial support and knowledge. I would like to thank all of the ITT staff for their work and in particular Mr. Chris Moses, Dr. Lei Qian, and Mrs. Patrice Hill. I have enjoyed my time with ITT and I am extremely grateful for the opportunity to be a fellow. Thank you to Mrs. Rebecca Berger and Mrs. Jaime Piszczek for their advice, help, and time.

Finally, I would like to say a special thank you to my family for all of their love and support. I could not have done it without you.

# TABLE OF CONTENTS

<b>LIST OF FIGURES .....</b>	<b>VII</b>
<b>LIST OF TABLES .....</b>	<b>IX</b>
<b>CHAPTER 1: INTRODUCTION .....</b>	<b>1</b>
1.1 PURPOSE OF RESEARCH .....	1
1.2 CHALLENGES .....	1
1.3 RESEARCH OBJECTIVES .....	2
<b>CHAPTER 2: LITERATURE REVIEW .....</b>	<b>4</b>
2.1 PROCESS FUNDAMENTALS .....	4
2.1.1 <i>The Langmuir-Blodgett Technique</i> .....	4
2.1.2 <i>Electrostatic Self-assembly</i> .....	5
2.1.3 <i>Deposition Conditions</i> .....	7
2.1.4 <i>Advantages and Disadvantages of Layer-by-Layer Assembly</i> .....	9
2.2 SURVEY OF SUBSTRATES USED .....	11
2.2.1 <i>Influence of Substrate Characteristics</i> .....	12
2.2.2 <i>Polymers as Substrates for Layer-by-Layer Deposition</i> .....	13
2.2.3 <i>Surface Modification Techniques</i> .....	15
2.3 SURVEY OF POLYELECTROLYTES USED .....	16
2.3.1 <i>Description of Polyelectrolyte Adsorption</i> .....	16
2.3.2 <i>Synthetic Polyelectrolytes Used</i> .....	17
2.3.3 <i>Modified and Natural Polyelectrolytes</i> .....	19
2.4 SURVEY OF ANALYSIS TECHNIQUES .....	20
2.4.1 <i>Fourier Transform Infrared Microscopy</i> .....	21
2.4.2 <i>X-ray Photoelectron Spectroscopy</i> .....	22
2.4.3 <i>Transmission Electron Microscopy</i> .....	23
<b>CHAPTER 3: EXPERIMENTAL.....</b>	<b>27</b>
3.1 SUBSTRATE SELECTION .....	27
3.1.1 <i>Cellophane Film</i> .....	27
3.1.2 <i>Cotton Fabric</i> .....	27
3.1.3 <i>Polyester Fabric</i> .....	28
3.2 SUBSTRATE CHARGING .....	28
3.2.1 <i>Chemical Treatment of Cotton</i> .....	28
3.2.2 <i>Plasma Treatment of Polyester</i> .....	30
3.3 POLYELECTROLYTE PREPARATION .....	33
3.4 DEPOSITION PROCESS .....	33
3.5 ANALYSIS TECHNIQUES .....	34
3.5.1 <i>FTIR-ATR</i> .....	34
3.5.2 <i>XPS</i> .....	35
3.5.3 <i>TEM</i> .....	36
<b>CHAPTER 4: RESULTS AND DISCUSSION.....</b>	<b>38</b>
4.1 VALIDATION OF DEPOSITION PROCEDURE .....	38
4.1.1 <i>FTIR-ATR Measurements</i> .....	38
4.1.2 <i>Validation of the Substrate Charging Procedures</i> .....	41
4.1.3 <i>XPS Measurements</i> .....	45

4.1.4 TEM Imaging .....	58
4.1.5 PET Analysis .....	63
<b>CHAPTER 5: CONCLUSIONS.....</b>	<b>66</b>
<b>CHAPTER 6: FUTURE WORK.....</b>	<b>67</b>
6.1 FUTURE SUBSTRATES .....	67
6.1.1 Substrate Charging .....	67
6.2 FUTURE POLYELECTROLYTES .....	68
6.3 FUTURE DEPOSITION PROCESSES .....	68
6.4 FUTURE ANALYSIS TECHNIQUES .....	69
<b>BIBLIOGRAPHY .....</b>	<b>71</b>

# LIST OF FIGURES

FIGURE 1-1. SEM IMAGE OF A COTTON FIBER. ....	2
FIGURE 1-2. SEM IMAGE OF A COTTON YARN SURFACE. ....	2
FIGURE 2-1. (A) SCHEMATIC OF THE FILM DEPOSITION PROCESS (B) MOLECULAR REPRESENTATION OF LAYER CREATION (C) TWO TYPICAL POLYELECTROLYTES: POLY(STYRENE SULFONATE) AND POLY(ALLYLAMINE HYDROCHLORIDE) [1]. ....	6
FIGURE 2-2. COMMON POLYELECTROLYTES USED DURING ESA.....	18
FIGURE 2-3. OPTICAL SCHEMATIC OF HITACHI HF-2000 TEM.....	25
FIGURE 2-4. VARIOUS GRID TYPES USED FOR TEM. ....	26
FIGURE 3-1. REACTION OF 3-CHLORO-2-HYDROXYPROPYLTRIMETHYL-AMMONIUM CHLORIDE. ....	29
FIGURE 3-2. PLASMATIC SYSTEMS, INC. PLASMA-PREEN 1.....	31
FIGURE 3-3. PLASMA-PREEN 1 REACTION CHAMBER.....	32
FIGURE 3-4. NICOLET NEXUS 470 FTIR.....	34
FIGURE 3-5. KRATOS AXIS ULTRA XPS SYSTEM. ....	35
FIGURE 3-6. SCHEMATIC OF KRATOS AXIS ULTRA XPS SYSTEM. ....	36
FIGURE 3-7. HITACHI HF-2000 TEM SYSTEM. ....	37
FIGURE 4-1. FTIR SPECTRA FOR A CELLOPHANE FILM. ....	39
FIGURE 4-2. FTIR SPECTRA FOR A KNIT FABRIC.....	40
FIGURE 4-3. (1) SCHEMATIC OF REFLECTION PATH WITHIN FTIR-ATR DEVICE (2) ENHANCED IMAGE OF KNIT FABRIC STRUCTURE SHOWING GAPS IN THE SURFACE. ....	41
FIGURE 4-4. C/O CPS RATIO AS A FUNCTION OF THE NUMBER OF DEPOSITED NANOLAYERS FOR THREE DIFFERENT CATIONIZATION PROCEDURES (A: 1.2, B: 1.55, C: 1.90). ....	42
FIGURE 4-5. N/O CPS RATIO AS A FUNCTION OF THE NUMBER OF DEPOSITED NANOLAYERS FOR THE THREE DIFFERENT CATIONIZATION PROCEDURES (A: 1.2, B: 1.55, C: 1.90). ....	43
FIGURE 4-6. S/O CPS RATIO AS A FUNCTION OF THE NUMBER OF DEPOSITED NANOLAYERS FOR THE THREE DIFFERENT CATIONIZATION PROCEDURES (A: 1.2, B: 1.55, C: 1.90). ....	44
FIGURE 4-7. C/O CPS RATIO AS A FUNCTION OF THE NUMBER OF DEPOSITED NANOLAYERS FOR CATIONIZATION PROCEDURE B (1.55 CAUSTIC:CR2000 MOLE RATIO).....	45
FIGURE 4-8. XPS SPECTRA FOR A CATIONICALLY CHARGED WOVEN COTTON FABRIC. ....	47
FIGURE 4-9. XPS SPECTRA FOR A CATIONICALLY CHARGED WOVEN COTTON FABRIC SUPPORTING 20 SELF-ASSEMBLED LAYERS WITH PAH BEING THE TOP LAYER.....	48
FIGURE 4-10. C/O RATIO FOR WOVEN CATIONIC COTTON SAMPLES COATED WITH 20 SELF-ASSEMBLED LAYERS. ....	49
FIGURE 4-11. N/O RATIO FOR WOVEN CATIONIC COTTON SAMPLES WITH 20 SELF-ASSEMBLED LAYERS. ....	51
FIGURE 4-12. N/O RATIO FOR WOVEN CATIONIC COTTON SAMPLES CONTAINING A PAH LAYER ON THE TOP.....	52
FIGURE 4-13. S/O RATIO FOR WOVEN CATIONIC COTTON FABRICS COATED WITH 20 SELF-ASSEMBLED LAYERS. ....	53
FIGURE 4-14. S/O RATIO FOR WOVEN CATIONIC COTTON SAMPLES CONTAINING A PSS LAYER ON TOP.....	54
FIGURE 4-15. N/S RATIO FOR WOVEN CATIONIC COTTON SUPPORTING 20 ALTERNATING LAYERS OF PSS/PAH.....	55
FIGURE 4-16. TEM IMAGE OF A COTTON FIBER COATED WITH A MULTILAYER PSS/PAH FILM.....	60
FIGURE 4-17. TEM IMAGE OF A COTTON FIBER COATED WITH A 20 LAYERS OF PSS/PAH. ....	61
FIGURE 4-18. HIGH RESOLUTION TEM IMAGE OF A CATIONIC COTTON FIBER COATED WITH A 20 LAYERS OF PSS/PAH. ....	62
FIGURE 4-19. XPS SPECTRA FOR KNIT PET FABRIC PLASMA TREATED WITH 100 HE. ....	63
FIGURE 4-20. XPS SPECTRA FOR KNIT PET FABRIC PLASMA TREATED WITH 100 HE SUPPORTING 20 SELF ASSEMBLED LAYERS. ....	64
FIGURE 4-21. N/S RATIO FOR PLASMA TREATED KNIT PET FABRIC SUPPORTING 20 ALTERNATING LAYERS OF PSS/PAH.....	65



**FIGURE 6-1. POSSIBLE AUTOMATED DEPOSITION SYSTEM.....69**

# LIST OF TABLES

<b>TABLE 3-1. FORMULATIONS EVALUATED FOR THE CHEMICAL CATIONIZATION OF THE COTTON SAMPLES. ....</b>	<b>30</b>
---	-----------

# **CHAPTER 1: INTRODUCTION**

## ***1.1 Purpose of Research***

One of the most commonly used methods of surface modification involves the use of multilayer thin films. Electrostatic self-assembly is one of several methods used to alter the surface characteristics of multilayer thin films. Electrostatic self-assembly has been used extensively to deposit nanolayers on substrates made of silica, mica, gold, glass, and titanium. Until now, textile materials have not been explored as substrates for this process. This research work is aimed at determining the appropriate conditions that will allow textile products to be used as substrates for the controlled deposition of nanolayers using electrostatic self-assembly.

## ***1.2 Challenges***

The electrostatic self-assembly process has not been implemented in textile materials as they pose a number of unique problems that are not found when using traditional substrates such as silicon wafers or gold particles. These problems include non-uniform surfaces and irregular shapes in yarns and fibers. In addition, the different types of fabric formation produce surfaces that are highly non-uniform. Examples of irregular surfaces can be seen in Figures 1-1 and 1-2.

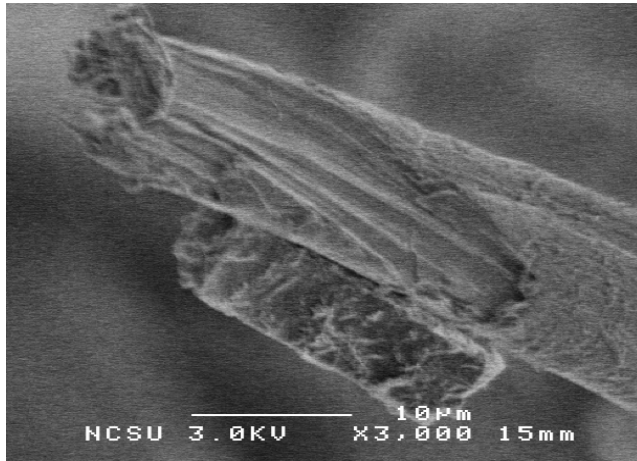


Figure 1-1. SEM image of a cotton fiber.

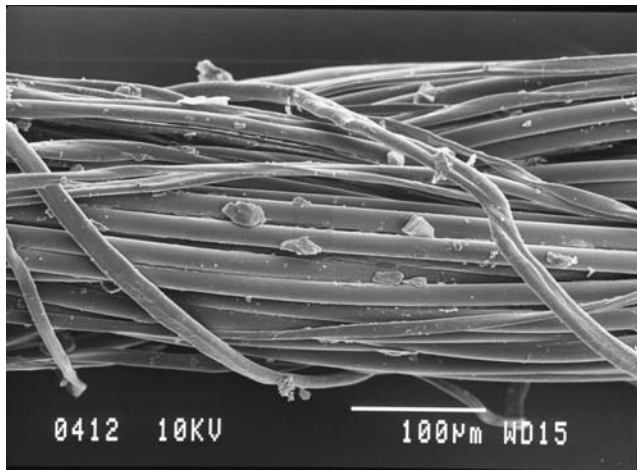


Figure 1-2. SEM image of a cotton yarn surface.

### **1.3 Research Objectives**

The primary objective of this research work is to validate the hypothesis that textile materials can be used as substrates for the controlled deposition of nanolayers using the electrostatic self-assembly method. There are also several secondary research questions that will be answered during this study including evaluation of physical and

chemical methods by which cotton and other textile fibers can be modified in order to support multilayer thin films.

Successful deposition of nanolayers onto textile by electrostatic self-assembly will provide a number of different benefits. This process will allow the surface of textile products to be controlled at a molecular level. The use of multilayer thin films will increase the surface functionality of the textiles without making major changes to the weight, bulk, or comfort of the material. In addition, it is possible that this deposition process would greatly reduce the number of chemicals normally needed for textile finishing. The self-assembly process is water-based and it does not require the use of expensive or hazardous solvents. The self-assembly process could also be easily adapted to current textile manufacturing techniques.

## **CHAPTER 2: LITERATURE REVIEW**

### ***2.1 Process Fundamentals***

Multilayer films made of polymeric materials have been studied for over the last 70 years. The interest in these types of films comes from the fact that they allow the creation of multicomposite molecular assemblies with great levels of reproducibility and exact molecular architectures. However, multicomposite structures require precise control of molecular orientation and organization at the nanoscale. The production of these multilayer structures is greatly influenced by the local chemical environment and as of today no single theory has been able to describe the process of self-assembly of thin films in its entirety [1].

#### **2.1.1 The Langmuir-Blodgett Technique**

Until the 1990s, the creation of molecularly controlled nanostructured films was dominated by the Langmuir-Blodgett (LB) technique. The LB technique consists of a system in which monolayers are formed on a non-solvent surface. The monolayers are then transported to a solid support. Kuhn and his group performed initial work on synthetic nanoscale heterostructures in the 1960s using the LB technique. These experiments were the first true nanomanipulations in that they allowed for the mechanical handling of individual molecular layers with a very high degree of precision [1].

As the LB technique was used more and more often, several disadvantages with the process became apparent. The LB technique requires special equipment that is often expensive and difficult to maintain. This technique is also limited by substrate selection

in regards to size and topology [1]. Because of the various problems with the LB technique, the development of a process capable of creating nanolayer films with well defined layers on any type of substrate has been a subject of much interest.

### **2.1.2 Electrostatic Self-assembly**

The electrostatic attraction between oppositely charged molecules provides an excellent basis for the creation of nanolayer films. This is due to the fact that it has the least steric demand of all chemical bonds [1]. Starting in the early 1990s, Decher's group began work on a realistic method of the electrostatic self-assembly of nanolayers [2-5]. Decher's group experimented with rod-like molecules with ionic groups at both ends, polyelectrolytes, and various other charged materials in aqueous solution [1]. The process developed by Decher and his colleagues has greatly increased in popularity since its introduction. This is a result of the method's simplicity and the fact that polyelectrolytes and charged nanoobjects can be used to create the nanolayers [6]. Figure 2-1 was used by Decher in his original publication in Science to describe the process. In this example, polyanions and polycations are alternately deposited on a positively charged surface. The phenomenon of strong electrostatic attraction between charged surfaces and oppositely charged molecules in solution is understood to be the dominant factor in the adsorption of polyelectrolytes [2, 7-10]. In theory, the adsorption of molecules possessing more than one equal charge allows for charge reversal on the surface. This behavior implies that (1) equally charged molecules will be repulsed allowing for adsorption self-regulation and restriction of the deposition to a single layer, and (2) an oppositely charged molecule can be adsorbed in a second step on top of the

first one. Both adsorption steps can be repeated cyclically to form multilayer structures on the surface of a substrate [1].

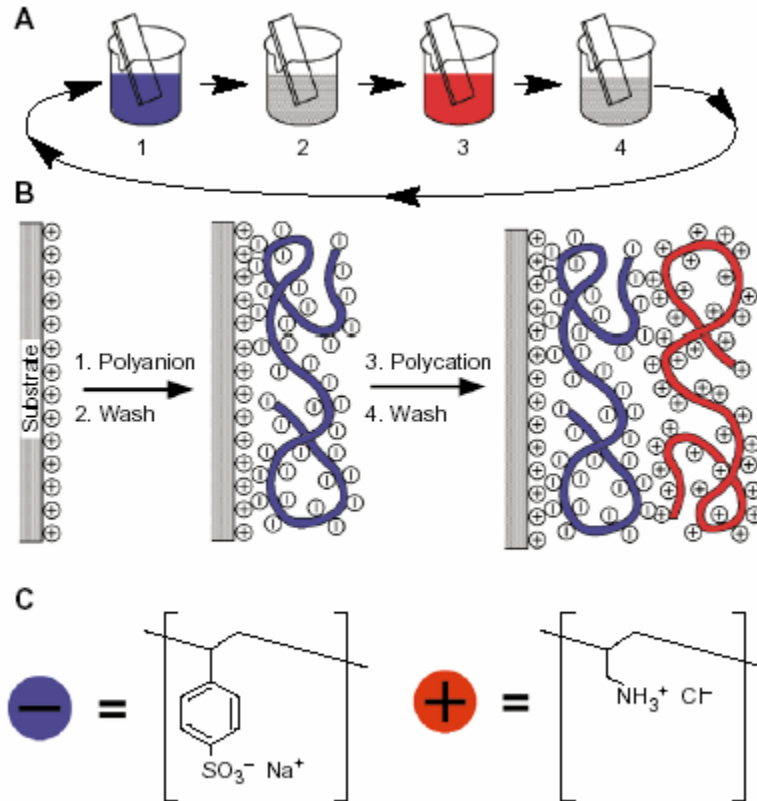


**Figure 2-1. (A) Schematic of the film deposition process (B) Molecular representation of layer creation (C) Two typical polyelectrolytes: poly(styrene sulfonate) and poly(allylamine hydrochloride) [1].**

Multilayer films may be composed of polyions, charged molecular objects, and/or colloidal objects. In theory, there are no limitations with respect to substrate size and topology due to the fact that the process involves adsorption from a solution. Nanolayer films have been created on objects of a variety of different sizes. Fig. 2-1B represents the buildup of a nanolayer film at the molecular level. A positively charged substrate adsorbs a polyanion. This is followed by a rinsing step in deionized water. The substrate, which now possesses a layer of a polyanion, then adsorbs a polycation. The



surface charge reversal that occurs with each adsorption step leads to the polyion conformation and layer interpenetration [1].

Decher's work determined that the use of polyelectrolytes was advantageous when compared to various other small molecules. While good adhesion of a layer to the base substrate requires a particular number of ionic bonds, the overcompensation of the surface charge by the incoming layer was found to be more dependent on the properties of the polymer than on those of the substrate. An additional benefit is that the polyelectrolytes can bridge over underlying defects. The conformation of a given polymer at the surface is then more dependent on the chosen polyelectrolytes and the adsorption conditions and less sensitive to changes on the surface of the substrate [1]. Numerous studies have shown experimental evidence of a linear increase of film thickness with the number of deposited layers independent of the nature of the initial substrate [11-16].

### **2.1.3 Deposition Conditions**

Nanolayer films are normally deposited using adsorbate concentrations of several milligrams per milliliter. While these concentrations are greater than those needed to reach a plateau in the adsorption isotherm, the excess makes sure that the solutions do not become depleted during the fabrication of many samples with multiple layers [1].

Washing steps are often used after the adsorption of each layer. The rinsing step is aimed at avoiding contamination of the next adsorption solution as well as to remove weakly adsorbed polymer layers, hence stabilizing the multilayer structure [14]. Adsorption times per layer can range from minutes for polyelectrolytes to hours for certain colloids.

The adsorption times depend on factors such as the molar mass, concentrations, and agitation of the polyelectrolyte solutions [1, 14].

Several different factors determine the composition of the multilayer film and the characteristics of the individual layers. The most easily measured property of an individual layer is its thickness. The thickness of a layer appears to be dependent on both the underlying surface and the deposition conditions. The nature and density of charged groups, their local mobility, and the surface roughness appear to have influence on the layer thickness. Operational factors such as concentration, adsorption time, ionic strength, temperature, rinsing time, dipping speed, drying time, also affect the thickness of the nanolayers [17]. For a given pair of strongly dissociated polycations and polyanions, the concentration of salt in the deposition solution appears to exert the strongest influence on the thickness of each polymer layer. The thickness of a nanolayer appears to be proportional to the salt concentration [13].

Self-assembly of nanoparticles to the oppositely charged substrate surface is mostly governed by adsorption and desorption equilibria. While the efficient adsorption of one monolayer of nanoparticles onto the oppositely charged substrate surface is the objective of the immersion step, preventing the desorption of the nanoparticles during the rinsing process is of equal importance. The optimization of the self-assembly in terms of maximizing the adsorption of nanoparticles from their dispersions and minimizing their desorption on rinsing requires the selection of proper stabilizers and careful control of the process kinetics [6, 18, 19].

#### **2.1.4 Advantages and Disadvantages of Layer-by-Layer Assembly**

The process of creating multilayer thin films using layer-by-layer adsorption has several advantages over other similar surface modification techniques such as the LB technique. One advantage of this process is that the film architecture is almost completely determined by the deposition technique. Another advantage of the layer-by-layer adsorption process is that a wide variety of different materials can be used to create the multilayer thin films hence creating truly multicomposite multilayer films [1]. Current examples of multicomposite films include structures that contain proteins, clay platelets, metals and gold colloids [1, 20-23].

Despite the fact that electrostatic self-assembly has become widely used in recent years, certain details of the process are still not clearly understood. For example, the existence of a minimum time needed to complete the deposition process has not been explained from first principles. The purpose of the intermediate washing and drying steps are also not well defined. Quantitative evaluation of the assembly process will be necessary to make electrostatic self-assembly a practical method [24]. Electrostatic self-assembly is also influenced by a variety of factors that can be difficult to control such as polymer entropy, charge transfer interactions, and hydrogen bonding [25]. No single theory has been developed to completely describe the deposition process. However, a variety of studies have been conducted that have helped to clarify many aspects of the electrostatic self-assembly method [7, 26, 27].

Layer-by-layer self-assembly using adsorption from solution is a very general method for the creation of multicomponent nanolayer films on solid substrates [1]. This

process has greatly increased in popularity since its introduction due to the method's simplicity and the fact that a great number of different polyelectrolytes and charged nanoobjects can be used to create the nanolayers [6, 7]. The multilayer films created using this process are made up of a number of layers in which each layer has its own individual structure and properties. The multilayer films can then be tailored to serve specific purposes [17]. Biological compounds, conducting polymers, light emitting polymers, and dyes can be manipulated by self-assembled nanolayers onto a suitable substrate [19, 28].

The ease of preparation and the high degree of versatility render self-assembled ultrathin films useful to a large variety of applications. Self-assembled films can function as barriers, with controllable levels of permeability, for gases, liquids, covalent molecules, ions and electrons. These properties have been used for the construction of insulators, passivators, sensors and modified electrodes. Self-assembled nanolayers are also suitable for the construction of devices based on molecular recognition. Molecules or nanoparticles within a self-assembled layer can be aligned spontaneously, or by changing the temperature, pressure and pH, or by the application of an electric or magnetic field. These characteristics permit the formation of superlattices with the desired architecture and allow the production of a number of photonic, electronic, magnetic and non-linear optical devices. The layer-by-layer self-assembly of insulators, conductors, and magnetic, ferroelectric and semiconductor nanoparticulate films allow the construction of molecularly controlled heterostructures. Control of the sizes and interparticle distances of the monodispersed nanoparticles within the self-assembled film

can also be used in optical applications [29-32]. Self-assembled nanolayers have been used to create polymer light emitting diode devices with improved performance characteristics when compared to traditional devices [33]. Controlling the various solution parameters such as surface charges and pair combinations has opened the possibility of creating new light sensitive materials and optical devices [34].

In addition to the applications and advantages listed above, the self-healing capability of electrostatic self-assembled nanolayers provides an increased tolerance to defects. This self-healing ability sets the electrostatic method apart from other self-organization techniques [6]. The electrostatic method can be used on substrates with non-uniform surfaces and compensates for defects caused during the adsorption process. It also allows the use of nanoparticles which might not necessarily provide smooth layers [24, 35]. The self-healing process is simply a result of the adsorption of multiple layers. As layers are added, defects are covered up or filled [36].

## ***2.2 Survey of Substrates Used***

Electrostatic self-assembly had been used to create nanolayer films on a number of different substrates including glass, quartz, mica, and silicone [6, 15, 18]. Gold and silver have also been used as base substrates [18, 37-40]. Both hydrophilic (fluorine, glass, and silicon) and hydrophobic (silanized glass) substrates have been successfully used to support nanolayer thin films [41]. The choice of substrates has often been determined by their convenience for different analysis techniques. Glass and quartz are used so that they can be analyzed using UV-VIS spectroscopy and optical microscopy [6]. Silicon wafers can be used for ellipsometric studies [21, 42]. The smooth surfaces

of substrates such as quartz and glass also make them well suited for X-ray reflectivity studies [15, 16, 43].

### **2.2.1 Influence of Substrate Characteristics**

Each of the different types of substrates differs in regards to their topology, smoothness and roughness. However, due to the characteristics of the layer-by-layer deposition technique, the adsorption of the materials used depends only on the surface charge of the structure [44].

The deposition of a film depends on the polyelectrolytes being used and the adsorption conditions. Therefore, the amount of polyelectrolyte adsorbed during the first deposition step depends on the substrate used and that substrate's surface charge [4, 45-49]. The amount of adsorbed polymer normally increases for the first five deposition steps before reaching a more constant level [13, 30]. At the same time, the average chemical composition of the surface of the films also becomes constant after the first five depositions [45]. The surface charge of the substrate determines how long it takes to reach this constant level. However, constant growth is eventually reached despite the substrate characteristics as long as the polyelectrolytes complement one another creating an electrostatic equilibrium [36, 46, 50].

Previous research has shown the influence of surface charge on the deposited layers. Fou and Rubner used microscopic glass slides with hydrophilic, hydrophobic, negatively charged, and positively charged surfaces as substrates. The surface charge of the substrates was found to have a great influence on the deposition time, layer thickness, and layer uniformity [51]. While previous research has clearly shown the importance of

the surface charge of the substrate, the characteristics of the structure itself have very little effect on the adsorption of the individual layers. The process allows various substrates of different sizes and shapes to be covered by ordered films of molecular thickness [44].

### **2.2.2 Polymers as Substrates for Layer-by-Layer Deposition**

Much of the early work involving the layer-by-layer assembly process used inorganic substrates such as quartz and silicone since it was thought that the process required flat clean surfaces [16, 22, 25]. Later reports began looking at using polymer films and other organic materials as substrates for the electrostatic deposition of nanolayers [52, 53]. Further research has looked at using a number of different polymer films as substrates for the deposition process. These polymers include poly(propylene), poly(isobutylene), poly(styrene), poly(methyl methacrylate), poly(ethylene terephthalate), poly(phenylene oxide), and poly(ether imide) [45].

Delcorte and others looked at the deposition of polyelectrolyte layers onto polymer films. Surface analysis techniques showed that alternate polyelectrolyte thin films could be built up on polymer substrates. The series of polymer supports tested included poly(propylene), poly(isobutylene), poly(styrene), poly(methyl methacrylate), poly(ethylene terephthalate) (PET), poly(phenylene oxide), and poly(ether imide). It was found that the best substrate for supporting multilayers was semi-crystalline PET films. Results of the study showed that polymer substrates containing carbonyl groups and/or benzene rings performed better than the other substrate choices [45].

Of particular interest to the textile industry are studies that used poly(ethylene terephthalate) film as a substrate for the self-assembly of nanolayers. PET can be surface modified by a variety of techniques including plasma, corona discharge, ion beam, laser treatment, photo-initiated graft polymerization, saponification, aminolysis, reduction, and entrapment of poly(ethylene oxide). PET is a suitable substrate for several reasons. It contains carbonyl groups that are capable of hydrogen bonding. The surface can be readily hydrolyzed to introduce carboxylic acid, as well as alcohol, functionality that can support negative charge (PET-CO<sub>2</sub><sup>-</sup>) in a sufficiently basic solution. The surface can react with polyamines to incorporate amine functionality that can support positive charge (PET-NH<sub>3</sub><sup>+</sup>) in a nonbasic solution [11].

Chen and McCarthy conducted a study involving the modification of PET with layer-by-layer deposition in 1996. Poly(sodium styrenesulfonate) and poly(allylamine hydrochloride) were used as polyelectrolytes for surface modification. These particular polyelectrolytes were used because of their extensive use in previous studies on self-assembled nanolayers. The techniques of contact angle analysis and X-ray photoelectron spectroscopy were used for analysis and proved effective in indicating the structure of the outermost layers, the individual layer thicknesses, and the overall multilayer thicknesses [11].

X-ray photoelectron spectroscopy and contact angle data indicated that the layers were stratified and that the wettability of the multilayer assemblies could be controlled by the identity of the outer most polyelectrolyte layer. The individual layers created were extremely thin (2-6 Å). The thickness was affected by the substrate surface chemistry



and it was confirmed that the thickness of each layer could be controlled by adjusting the ionic strength of the polyelectrolyte solutions. The stoichiometry of the deposition process (ammonium ion: sulfonate ion ratio) was also affected by the substrate chemistry and solution ionic strength. This indicated that the layer-by-layer deposition process was quite forgiving and could be done under a variety of conditions. Peel tests showed that the multilayer assemblies had good mechanical properties. No failures were observed in the multilayers. These experiments indicated that layer-by-layer deposition was a viable tool for polymer surface modification and that PET fibers/fabrics could eventually be used as a base substrate for the electrostatic self-assembly process [11].

### **2.2.3 Surface Modification Techniques**

Several modification techniques are used to modify the amount of surface charge present on a substrate. These techniques can be used on both organic and inorganic substrates. Techniques for surface modification may be physical or chemical. Chemical modification techniques that have been used include surface patterning, photobleaching, or plasma treatment [5, 50, 54, 55]. Methods of physical modification consist of using Langmuir-Blodgett films or layers of charged polyelectrolytes as primers for the deposition of multilayers [4, 56-58].

A number of studies have been conducted in order to add functionality to cotton fibers. Numerous chemicals have been used for this purpose. One method of improving the cationic nature of cotton is to create cationic sites on the fibers through the use of controlled epoxy-based chemical reactions. It has been previously reported that reacting cotton with 2,3-epoxypropyltrimethylammonium chloride forms cationic charges on the

surface of the fibers. While this process was originally developed to improve the affinity of cotton for anionic dyes, it will be used during this work to provide the cotton fabric with a positive surface charge aimed at supporting an anionic polyelectrolyte layer [59].

## ***2.3 Survey of Polyelectrolytes Used***

### **2.3.1 Description of Polyelectrolyte Adsorption**

Aqueous solutions of polyelectrolytes are commonly preferred for depositing layer-by-layer assemblies. However, organic solvents have proven to be useful as well. The use of polyelectrolytes can be easily adapted to automated systems and is not restricted by the size or shape of the substrates. The use of polyelectrolytes allow the creation of multiple electrostatic interactions between the polymers and the substrate improving adhesion to the substrate as well as cohesion between the layers [6].

Since the electrostatic self-assembly method is mainly based on the attraction of opposite charges, it is necessary that the layer-forming compounds have at least a minimal number of charged groups. Below this minimum charge, the layer-by-layer deposition process no longer works. Thin films made from polyelectrolytes require that the deposition parameters be very carefully controlled. Various other strong interactions can help to reduce the minimum charge required for the layers to be adsorbed [12, 46, 60-63]. Past studies have led to the theory that large hydrophobic fragments found in polyelectrolytes would be detrimental to the layer-by-layer deposition technique as they reduce the charge density and can interfere with ion-ion interactions. Experiments involving weak polyelectrolytes supported this theory [14, 64]. These results led to the belief that the minimum charge of the polyelectrolytes was a determining factor in the

layer by layer process. However, more recent studies have successfully used polyelectrolytes with very low charge densities [65].

### **2.3.2 Synthetic Polyelectrolytes Used**

A large number of polyelectrolytes have been used to create a variety of nanostructured thin film coatings [1, 19, 66-68]. Some of these polyelectrolytes include poly(ethyleneimine), poly(allylamine), poly(diallyldimethylammonium chloride), poly(styrene sulfonate), poly(vinyl sulfate), poly(acrylic acid), and poly[*N*-vinyl-(4-(39-carboxy-49-hydroxyphenylazo) benzene sulfonamide)]. Figure 2-2 shows some of the most used polyelectrolytes [6].

One of the most studied and well understood systems is the poly(allylamine) and poly(styrene sulfonate) system [11, 15, 69-71]. A number of more complex, functionalized polyelectrolytes have also been used based on their ability to form structured coatings, and whether or not they can enable secondary chemical modifications. One of the greatest advantages of the layer-by-layer deposition technique is that almost any polyelectrolyte can be used as long as the appropriate oppositely charged partner polyelectrolyte is chosen [6].

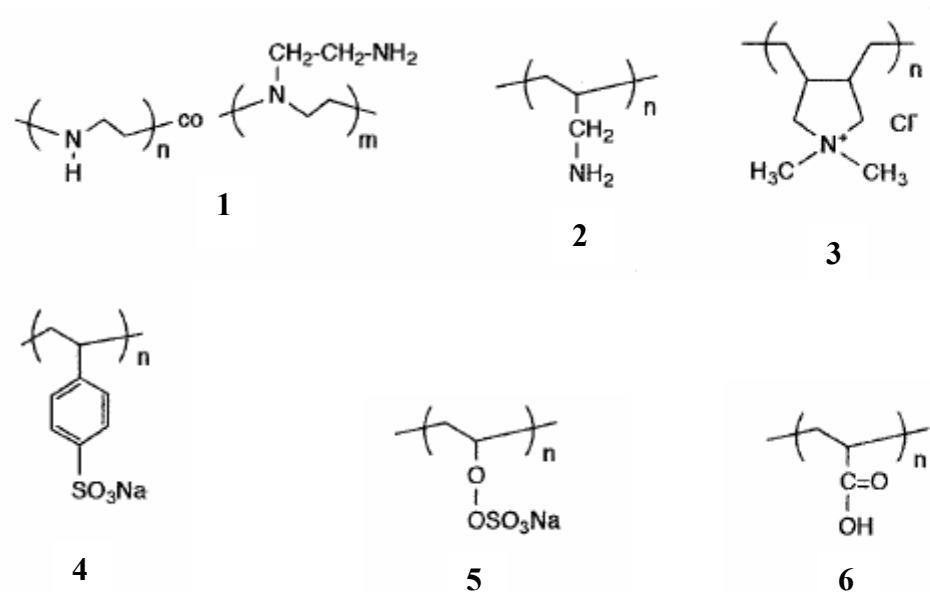


**Figure 2-2. Common Polyelectrolytes used during ESA (1) poly(ethyleneimine) (2) poly(allylamine) (3) poly(diallyldimethylammonium chloride) (4) poly(styrene sulfonate) (5) poly(vinyl sulfate) (6) poly(acrylic acid) [6].**

A large number of functional polymers have also been studied including electrical and ionic conducting and light-emitting polymers [72-81]. Past experiments have also used non-conjugated redox-active polymers, reactive polymers, and polymeric complexes [82-91]. Standard polyelectrolytes modified with small numbers of functional groups have also been used for labeling purposes and for molecular recognition studies [50, 92-94]. Polyelectrolytes labeled with dyes and fluorescent probes have been used in an effort to better understand the adsorption of the layers [30, 45, 95-100]. Complementary chromophores have also been used to monitor multilayer adsorption on real time basis via UV-VIS spectroscopy and colorimetric methods [6].

### 2.3.3 Modified and Natural Polyelectrolytes

Charged nanoobjects such as stable colloidal dispersions of charged silica, metal oxides, microcrystallites, and metal colloids have been deposited using the layer by layer technique [21, 95, 101-110]. Charged nano-objects are usually referred to as rigid polyelectrolytes.

Most of the scientific work performed in the area of electrostatic self-assembly has used polyelectrolytes that are in a fully charged state. Poly(styrene sulfonate) and poly(allylamine hydrochloride) are examples of polyelectrolytes that are often deposited at pH values less than 7.0. Recent studies have looked at multilayers composed of weak polyelectrolytes. The charge density of these polyelectrolytes can be controlled by adjusting the pH values of the solutions [19, 111]. Weak polyelectrolytes such as PAA and PAH allow for a more precise control over the physical characteristics of the multilayers. Weak polyelectrolytes can be deposited with a high percentage of the chains making loops and tails under pH conditions of incomplete charge. This is in contrast to strong polyelectrolytes which often deposit as molecularly thin layers (about 5 Å). Layer thicknesses greater than 80 Å have been achieved when using weak polyelectrolyte solutions of PAA/PAH [19, 111].

Natural polyelectrolytes can also be used for layer-by-layer electrostatic self-assembly. Nucleic acids, proteins, and polysaccharides have been used to create multilayer thin films [112-114]. Studies involving these polyelectrolytes looked at the biological function of films and their ability to simulate biological processes. The main

advantage is that the assembly of proteins via layer-by-layer deposition does not require chemical modification and should in theory maintain normal protein behavior [115-117].

The physical characteristics of the surface of a substrate do not appear to have a large effect on the deposition of multilayer films as long as the ionic groups are accessible. Cyclic compounds, dendrimers, and hyperbranched polyelectrolytes have all been used with success [42, 118-120]. Poly(ethyleneimine), which is a highly branched polymer, has been used frequently in studies involving layer-by-layer assembly [6].

To summarize, the layer-by-layer deposition method can be utilize a wide range of polyelectrolytes as long as a suitable partner polyelectrolyte is selected. When compared to chemical methods of creating multilayer thin films, the electrostatic self-assembly method is much more versatile. A vast amount of synthetic and natural polyelectrolytes can be used to create the films. Alternatively, charged nanoobjects can be used instead of polyelectrolytes. This further increases the list of materials suitable for deposition [6].

## ***2.4 Survey of Analysis Techniques***

Since the introduction of the electrostatic self-assembly method, a variety of techniques have been used to analyze self-assembled nanolayers. Recent work by Akin and his research group illustrates the use of the most common analysis techniques namely x-ray photoelectron spectroscopy (XPS), x-ray reflectivity, and atomic force microscopy (AFM) [121]. Self-assembled nanolayer films have also been characterized using infrared spectroscopy, UV-VIS spectroscopy, ellipsometry, planar optical wave guide systems, and quartz crystal microgravimetry (QCM) [18]. Surface plasmon

resonance (SPR) measurements have also been used to characterize multilayer thin films adsorbed onto gold and other noble metal substrates. SPR monitors the reflectivity of an incident light beam from a thin film that is attached to a glass prism as a function of the incident angle [122]. Gel permeation chromatography, nuclear magnetic resonance (NMR) spectroscopy, and end group titration. NMR, infrared (IR), and XPS spectroscopy are primarily used to determine the chemical functionality of the end groups. FTIR and XPS spectroscopy in particular have been used with success when analyzing multilayer thin films [123].

#### **2.4.1 Fourier Transform Infrared Microscopy**

Fourier Transform Infrared microscopy (FTIR) combines a microscope with an infrared spectrometer to create an instrument that allows detection of individual chemical species in specific spatial regions. FTIR constructs a species map for a sample by combining spatial specificity with information on its chemical constitution. This is done by measuring the IR spectrum of the sample at a number of different points. An entire area of the sample can be mapped point-by-point [124].

Internal reflection spectrometry, which is also called attenuated total reflectance infrared (ATR/IR) spectrometry, can provide valuable information related to the chemical structure of a sample. Mid-infrared spectra can be gained by pressing small pieces of the sample against an internal reflection element (IRE). IR radiation is then focused onto the end of the IRE. Light enters the IRE and reflects down the length of the crystal. The IR radiation then penetrates a short distance ( $\sim 1 \mu\text{m}$ ) from the surface of the IRE into the polymer sample [124].

This technique provides information on the chemical bonds present on the surface of the sample. Adsorption of radiation correlates to the fundamental vibrations of chemical bonds in the mid-infrared spectrum. FTIR-ATR provides data on the presence or absence of certain functional groups and shifts in the frequency and changes in the intensity of absorption bands relate to changes in the chemical structure of the surface of the sample being studied. FTIR-ATR spectrometry can also be used to determine changes in surface chemistry after special chemical or physical treatments are applied [124].

#### **2.4.2 X-ray Photoelectron Spectroscopy**

XPS is also known as Electron Spectroscopy for Chemical Analysis (ESCA). It is a non-destructive surface sensitive technique. XPS provides quantitative surface chemical state information for all elements except hydrogen and helium. Since its establishment in the mid-1960s, XPS has become one of the most widely used surface analysis techniques. XPS provides quantitative compositional information for the top ten atomic layers of a sample surface. At the same time XPS gives data regarding the chemical states of the elements present on the surface of the sample [125].

XPS works by irradiating the sample with a beam of monochromatic soft x-rays. This results in photoelectric emission from the atoms in the sample. The kinetic energies of these electrons relate to the atom and the orbital from which they originate. The distribution of the kinetic energies is then measured by the electron spectrometer. Atomic orbitals from atoms of the same element in different chemical environments are found to possess slightly different binding energies. These differences, which are



referred to as chemical shifts, are a result of the variations in electrostatic screening experienced by core electrons as the valence and conduction electrons are drawn towards or away from the specific atom. Differences in oxidation state, molecular environment and co-ordination number all provide different chemical shifts. Photoelectron binding energy shifts are, therefore, the principal source of chemical information [126].

It has been amply reported that the precision in determining the thickness of a single layer within multilayer film is often poor because of the apparent interfacial roughness between the different layers. Consequently, the formed multilayer films may have a disordered and intermeshed structure without clear distinction between individual layers [71]. This problem would become evident when evaluating the layers deposited on textile substrates such as those used in this research project.

### **2.4.3 Transmission Electron Microscopy**

Transmission electron microscopy (TEM) is an imaging technique that places a beam of electrons onto a sample. This causes an enlarged version of the sample to appear on a fluorescent screen. TEM systems are based on the principles of light microscopes. The maximum resolution that a microscope can see is determined by the wavelength of the photons that are used to probe the sample. Objects smaller than the wavelength being used can not be viewed. Visible light has wavelengths between 400-700 nm, which is larger than many items of interest. Other wavelengths can be used but experience problems with absorption, focusing, and interaction with the sample being viewed [127].

Electrons have properties of waves and particles. Their wave-like properties cause them to behave like a beam of radiation in certain circumstances. Electron

wavelength is defined by their energy and can therefore be adjusted by the use of accelerating fields. The wavelength of the electrons can be much smaller than that of light but can still react with the sample due to their electrical charge. With the use of electrical and magnetic fields, the electrons can be focused onto the sample. This electron beam provides much higher resolution than light microscopes and at the same time improves the depth of vision [127]. Figure 2-3 provides a schematic of how the TEM system used for this research works.

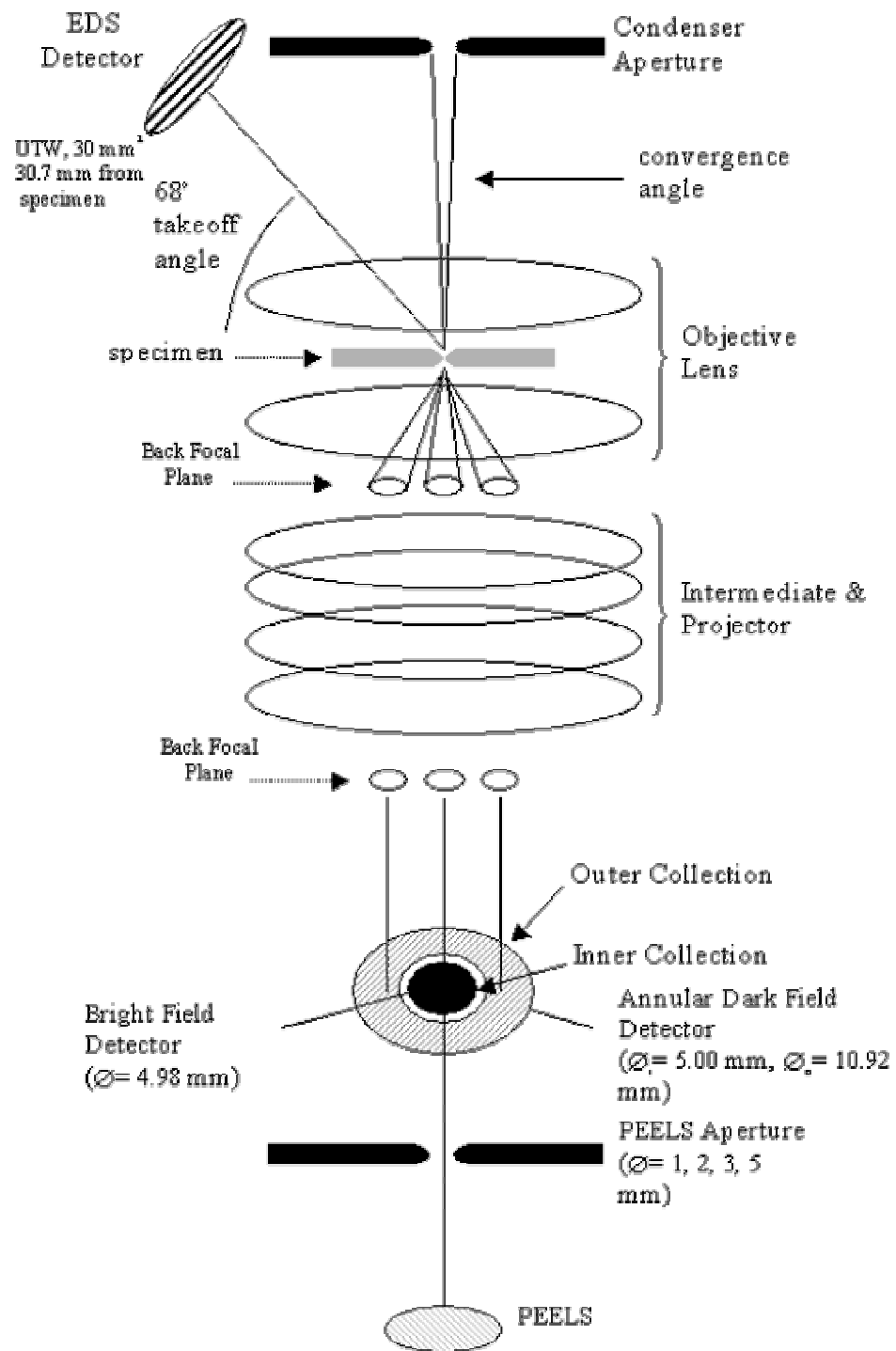
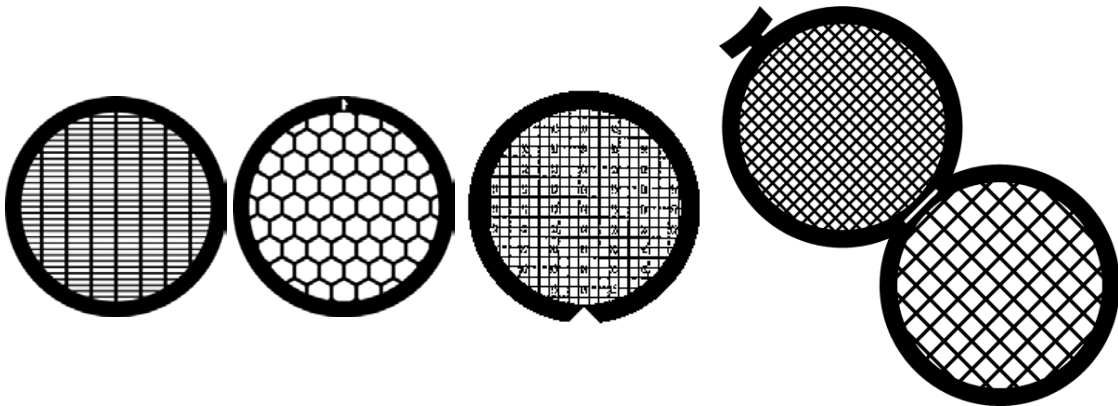


Figure 2-3. Optical schematic of Hitachi HF-2000 TEM [128].

Samples used for TEM are normally extremely thin. Film samples are often analyzed. Specimens must be thin enough that the electron beam can pass through it. In addition the specimen must be capable of withstanding the vacuum created within the device. Most samples used are inorganic and non-biological [129]. TEM samples are generally mounted onto holders called grids. These grids come in a number of different shapes and sizes and can be seen in Figure 2-4. Grids may also be made of different materials such as copper, nickel, and gold. TEM samples are mounted to the grids in a variety of ways. Various types of adhesives from general super glue to specially developed products such as M-bond can be used with TEM samples.



**Figure 2-4. Various grid types used for TEM.**

## **CHAPTER 3: EXPERIMENTAL**

### ***3.1 Substrate Selection***

Since the electrostatic self-assembly technique has not been used in textile substrates, preliminary experiments for this research project were conducted using polymer films in order to evaluate the feasibility of the deposition technique.

#### **3.1.1 Cellophane Film**

Cotton fabrics were initially identified as potential substrates for the deposition of self-assembled nanolayers. As a preliminary step, cellophane films were used to evaluate the feasibility of the deposition technique due to its chemical structure similarity with cotton. Food grade cellophane films (LS273103 SJP Cellulose) were purchased from Goodfellow, Inc. (Devon, PA). The films used had a thickness of 0.021 mm.

#### **3.1.2 Cotton Fabric**

Two types of mercerized and bleached cotton fabrics were used as substrates for this study: knit and woven. The fabrics were cut into approximately 10 inch x 20 inch pieces before being treated. These large pieces were then cut into smaller 1 inch x 1 inch squares before the deposition process. The woven cotton structure used was 3 x 1 twill.

### **3.1.3 Polyester Fabric**

The polyester samples used in this study were knit fabrics. The fabric (scoured, TIC 729, 95-53) was obtained from SDL Textile Innovators Corporation. The samples were cut into approximately 1 inch x 1 inch squares and labeled before being treated.

## **3.2 Substrate Charging**

While the cotton samples used in this project were treated chemically, a low temperature He-O<sub>2</sub> plasma was used to impart charge to the polyester samples.

### **3.2.1 Chemical Treatment of Cotton**

Recent work by Hauser and collaborators introduced a process capable of modifying cotton fabric in order to improve its affinity for anionic dyes. This process relies on reacting cotton with 2,3-epoxypropyltrimethylammonium chloride. 2, 3 epoxypropyltrimethylammonium chloride was prepared in aqueous solution by the reaction of 3-chloro-2-hydroxypropyltrimethylammonium chloride with alkali. This compound reacts with alcohols under alkaline conditions to form ethers. Once in contact with cotton it imparts a cationic charge on its surface [59]. A schematic of the chemical reaction mechanism can be seen in Figure 3-1 below.

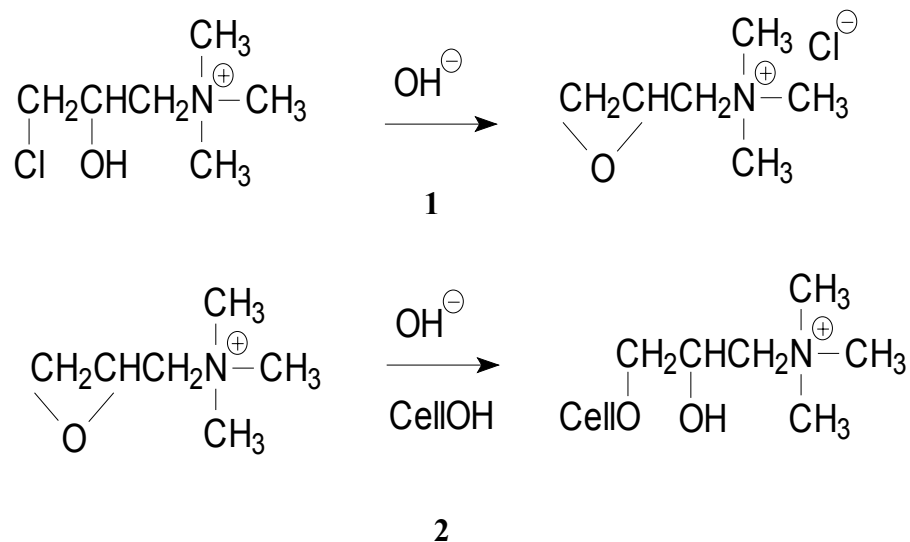


**Figure 3-1. (A) Reaction of 3-chloro-2-hydroxypropyltrimethylammonium chloride with alkali to create 2,3-epoxypropyltrimethylammonium chloride (B) Reaction of 2,3-epoxypropyltrimethylammonium chloride with alcohol and cellulose to form cationic cotton [59].**

Three different formulations of 2,3-epoxypropyltrimethylammonium chloride were evaluated. The treatment formulas differed in their ratios of caustic to 3-chloro-2-hydroxypropyltrimethylammonium chloride (CR2000). The ratios used can be seen in Table 3-1. After the reactant was prepared, it was loaded into a padder and the fabric was then immersed in the solution. The solution was pad applied to the cotton fabric at 100% wet pick-up. After treatment, the fabric was placed in Ziploc bags and remained at room temperature for 24 hours. After 24 hours, the fabric was dried in a commercial dryer to remove any remaining moisture. After the fabric was completely dry, it was cut into 1 inch x 1 inch samples and labeled. Random samples were dyed using anionic dyes to ensure that the process had placed a cationic charge on the surface of the fabric. The samples were then placed in Ziploc bags until the deposition process was initiated.

**Table 3-1. Formulations evaluated for the chemical cationization of the cotton samples.**

	Caustic:CR2000 mole ratio		
	<b>1.2</b>	<b>1.55</b>	<b>1.9</b>
G CR2000	100	100	100
G 50% NaOH	35.2	45.5	55.8
mL water	200 mL	200 mL	200 mL

### **3.2.2 Plasma Treatment of Polyester**

Helium and oxygen plasma mixtures were used to modify the surface of the polyester samples. Helium and oxygen mixtures have gained interest in plasma treatments thanks to their ability to produce surface oxidation at the same time as a crosslinking reaction. Together, these two mechanisms are expected to produce a reactive surface with good stability in regards to ageing [130].

A Plasmatic Systems, Inc. (North Brunswick, NJ) PLASMA-PREEN 1 was used to plasma treat the polyester samples. The system can be seen in Figure 3-2 below. The PLASMA-PREEN 1 is a plasma etching system. The system is manufactured from a microprocessor controlled microwave oven and uses the built in digital controls of the oven. The system was equipped with a quartz-made barrel type process chamber that measured 4.1 inches in diameter and 6.0 inches long as seen in Figure 3-3.



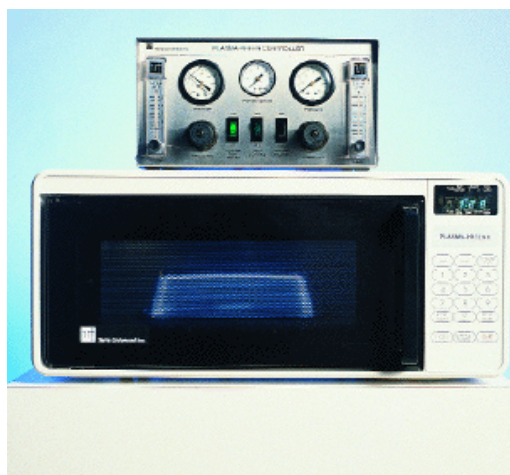


**Figure 3-2. Plasmatic Systems, Inc. PLASMA-PREEN 1.**

The PLASMA-PREEN 1 system works by flowing the process gas into the process chamber at reduced pressures (1 to 5 torr). The plasma discharge is excited by the microwave energy from the microwave oven. The process creates ionized gas species and free radicals within the gas. These active species then react with the sample in the chamber. The PLASMA-PREEN 1 has a power range from 100 up to 750 watts and operates at 2.45 GHz. The polyester fabric was placed into the glass reactor and then treated using different mixtures of helium-oxygen. Batches of 20 1 inch x 1 inch samples were placed in the process chamber and then treated.



**Figure 3-3. PLASMA-PREEN 1 reaction chamber.**

Helium and oxygen were provided by Machine & Welding Supply Company (Raleigh, NC). Aalborg mass flow-meter/controllers were used to measure and control the gas flow rate. The pressure within the chamber was measured with a Supco VG64 digital vacuum gauge. The glass reactor was pumped using a Precision Scientific vacuum pump to a typical pressure of 1.0 torr.

Four different gas mixtures were used: (1) 100% He (2) 20% He / 80% O (3) 50% He / 50% O (4) 80% He / 20% O. The 100% He samples were treated for 1 minute with a power level of 10 and a duty cycle of 10. The samples for the remaining three mixtures were treated for 1 minute with a power level of 10 and a duty cycle of 0. The change in duty cycle was implemented to prevent thermal degradation of the samples. PET film was initially used to test feasibility of the technique and to determine the optimum operation conditions. Untreated PET film is hydrophobic while plasma treated PET film becomes hydrophilic. The settings on the PLASMA-PREEN 1 were adjusted until the PET film samples exhibited hydrophilic characteristics by measuring the contact angle of

water on the film. After the settings were verified, the polyester fabric was treated.

Three sets of twenty fabric samples were prepared for each mixture. After treatment, the polyester samples were placed in Ziploc bags for storage until they were used.

### ***3.3 Polyelectrolyte Preparation***

Poly(sodium 4-styrene sulfonate) and poly(allylamine hydrochloride) were used in this study. Prior studies have shown that these two particular polyelectrolytes are able to create self-organized layers on planar substrates that can be analyzed using techniques such as FTIR and XPS [8, 11, 131].

Poly(sodium 4-styrene sulfonate) (PSS),  $M_r$  70,000, and poly(allylamine hydrochloride) (PAH),  $M_r$  70,000, were purchased from Aldrich (St. Louis, Mo) and used as received. Solutions of the polyelectrolytes were prepared at concentrations of 5 mM/L.

### ***3.4 Deposition Process***

Thirty-two glass petri dishes were used for the deposition. The dishes were laid out in an array of four by eight dishes in order to facilitate the deposition process. The first row of dishes contained the anionic polyelectrolyte solution, PSS; the second and fourth rows contained deionized water for rinsing; and the third row contained the cationic polyelectrolyte solution, PAH. The petri dishes were filled to a level that would immerse the different fabric samples. Solutions were rinsed out and replaced when they became cloudy. Unused dishes were kept covered in order to prevent evaporation and contamination.

Rinsed samples were placed in the first PSS dish for five minutes. Using tweezers the sample was then moved to the next dish containing deionized water. The sample remained in the rinsing dish for five minutes and then was moved to the next dish containing PAH. After five minutes, the sample was transferred to the next dish containing deionized water to be rinsed for five minutes again. The process was continued until the desired number of layers was achieved. Samples were dried at room temperature for a period of 24 hours before being placed in Ziploc bags for storage.

### **3.5 Analysis Techniques**

#### **3.5.1 FTIR-ATR**

A Nicolet Nexus 470 FTIR spectrophotometer, shown in Figure 3-4, was used to obtain infrared spectra of the sample surfaces. The Nexus is equipped with an OMNI-ATR sampler with a germanium crystal and an incident angle of 45°. It provides a 10 micron viewing area. The spectra were taken over a range of 4000 to 700  $\text{cm}^{-1}$  with a resolution of 2  $\text{cm}^{-1}$  and 64 scans.



**Figure 3-4. Nicolet Nexus 470 FTIR.**

### 3.5.2 XPS

XPS measurements were conducted using a Kratos AXIS Ultra spectrometer located at Duke University Shared Materials Instrumentation Facility. A picture of the system can be seen in Figure 3-5. The AXIS Ultra is equipped with an aluminum source and a spherical mirror analyzer working in spectrum mode. The total pressure in the main vacuum chamber during analysis was typically  $4 \times 10^{-7}$  torr.



**Figure 3-5. Kratos AXIS Ultra XPS system.**

Spectra were collected with the stage containing the samples at  $0^\circ$ . The take-off angle of the electrons was  $90^\circ$  and the angle of the incident X-rays hitting the sample was  $30^\circ$ . A schematic of the process can be seen in Figure 3-6. The chemical elements present on the samples were identified from a survey spectrum. Survey scans were of the spectrum type with an Al reference. The survey scans started at 1200 eV and ended at -5 eV taking 1 eV steps with a dwell time of 200 ms. High resolution scans were then performed around peaks of interest.

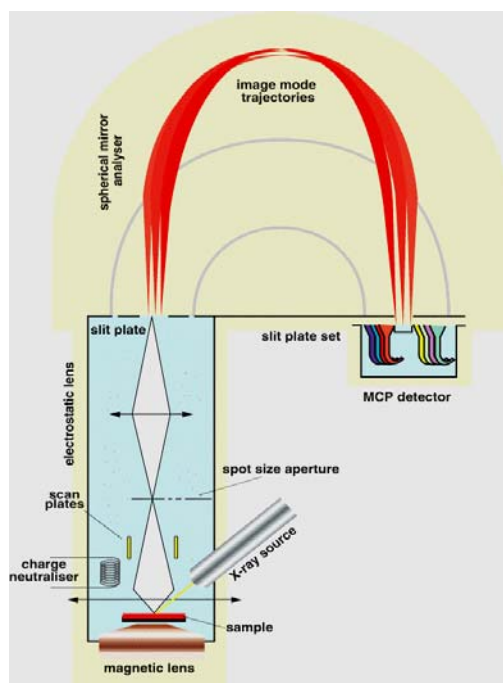
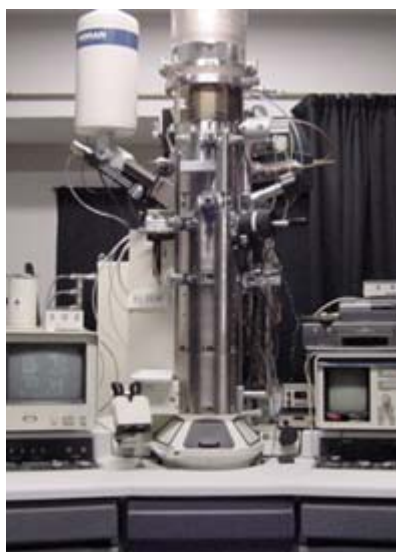


Figure 3-6. Schematic of Kratos AXIS Ultra XPS system.

### 3.5.3 TEM

TEM images were obtained using a Hitachi HF-2000 system, as seen in Figure 3-7. The HF-2000 uses a cold field emission electron source with an accelerating voltage of 200 kV. This type of source creates an electron beam with little energy spread and strong stability which allows high microscope resolution. The TEM system used is also equipped with an Advanced Microscopy Techniques XR-60B digital camera system for digital imaging. The resolution of the system is .10 nm (lattice) and .23 nm (point to point). The microscope is capable of a maximum magnification value of 1,500,000 X. 3 mm diameter samples are used in this device.



**Figure 3-7. Hitachi HF-2000 TEM system.**

Samples for TEM were prepared by pulling individual fibers from the fabric samples using tweezers. The fibers were attached to the TEM grids using different adhesives. Two types of copper grids were used, slot and mesh. The mesh grids used were 200 mesh (line/inch) and slot grids had a hole width of 1000 x 200  $\mu\text{m}$ . Loctite super glue gel was used to attach the fibers to the mesh grids. Glue was placed around the grid edges before the fibers were laid down. Another grid was then placed on top to create a grid sandwich. Fibers were placed on the slot grids using double sided tape. The tape was trimmed to fit the grids and the fibers were then placed. “Sticky grids” were also used to hold the fibers. These “sticky grids” were prepared by dissolving 30 mm of double sided tape in 20 mL of chloroform for approximately 15 minutes. The grids were then dipped in the adhesive solution to create a grid with an adhesive on it.

## CHAPTER 4: RESULTS AND DISCUSSION

### *4.1 Validation of Deposition Procedure*

A series of experiments were carried out to determine the reproducibility and accuracy of the deposition process. Samples of cellophane film, knit cotton fabric, and woven cotton fabric were prepared using the procedure described in the prior chapter. Polyelectrolytes (PSS and PAH) were then deposited onto the samples and the deposition process was assessed using FTIR-ATR, XPS and TEM.

#### **4.1.1 FTIR-ATR Measurements**

Figure 4-1 shows three different FTIR spectra for samples of cellophane film. The bottom spectrum corresponds to that of unmodified cellophane film, the middle spectrum to a sample that has been cationically charged, and the top spectrum to a sample having an outer layer of PAH. The deposition of PAH onto the cellophane was determined by monitoring the following peaks in the spectra:  $2923.15\text{ cm}^{-1}$  which indicate the presence of aliphatic hydrocarbons, at  $2853.55\text{ cm}^{-1}$  indicating the presence of  $\text{NH}_3^+\text{Cl}^-$ , and at  $1710$  and  $1740\text{ cm}^{-1}$  illustrating the presence of  $-\text{CH}_2\text{NH}_2$  groups in the outer polymer layer.



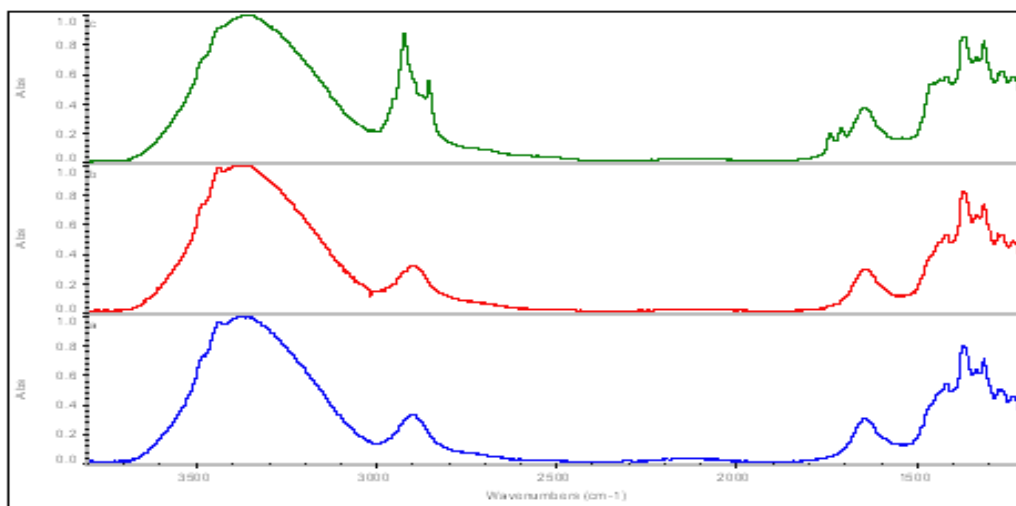


**Figure 4-1. FTIR spectra for a cellophane film: unmodified film on bottom, cationically charged in middle, film with a PAH layer on top.**

Figure 4-2 shows three different FTIR spectra for samples of knit cotton fabric.

The bottom spectrum is for the unmodified material, the middle spectrum is for that with a layer of PSS on top, and the top spectrum for that one with a layer of PAH on top.

Additional peaks can be detected when comparing the unmodified knit cotton sample to the samples with PSS and PAH on top. The spectrum for the sample with PSS on top shows the presence of p-substituted aromatic hydrocarbons at  $2920.93\text{ cm}^{-1}$  and of aliphatic hydrocarbons at  $2852.3\text{ cm}^{-1}$ . When the outermost layer was PAH (top spectrum), the presence of  $-\text{CH}_2\text{NH}_2$  groups was observed at  $1735.15\text{ cm}^{-1}$ .

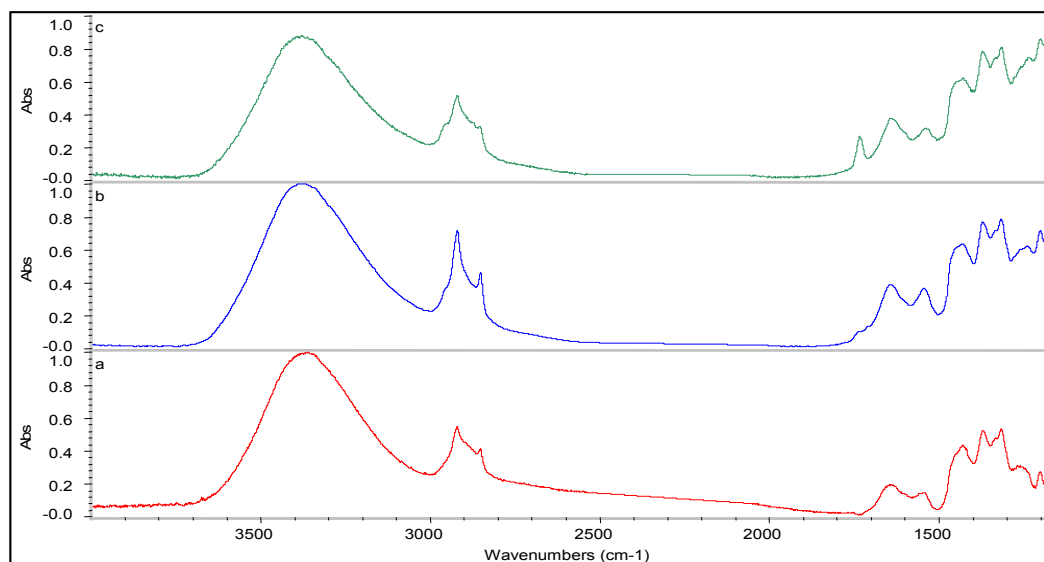


**Figure 4-2. FTIR spectra for a knit fabric: a.) unmodified fabric b.) fabric with a PSS layer, c.) fabric with a PAH layer.**

It was noted that the changes in the peaks in Figure 4-2 were not as significant as the changes evident in Figure 4-1. This difference may be the result of the nature of the knit cotton substrate. The knit cotton substrate has a large amount of open spaces within it. Textile products in general are very porous materials and this porosity results in poor sensitivity when using FTIR-ATR. The FTIR-ATR process works by measuring the energy reflected off of the surface of an object. Due to the porosity of the knit cotton samples, it is expected that a large number of air gaps exist between the sample and the crystal. This effect can be seen in Figure 4.3 below. Because of these non-definite results, this research work moved to use woven cotton fabrics as substrates.

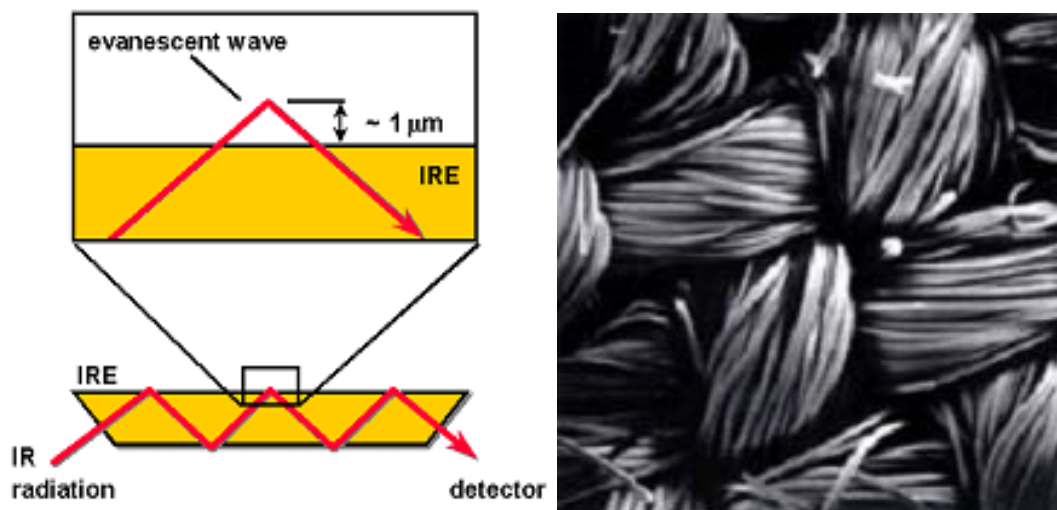
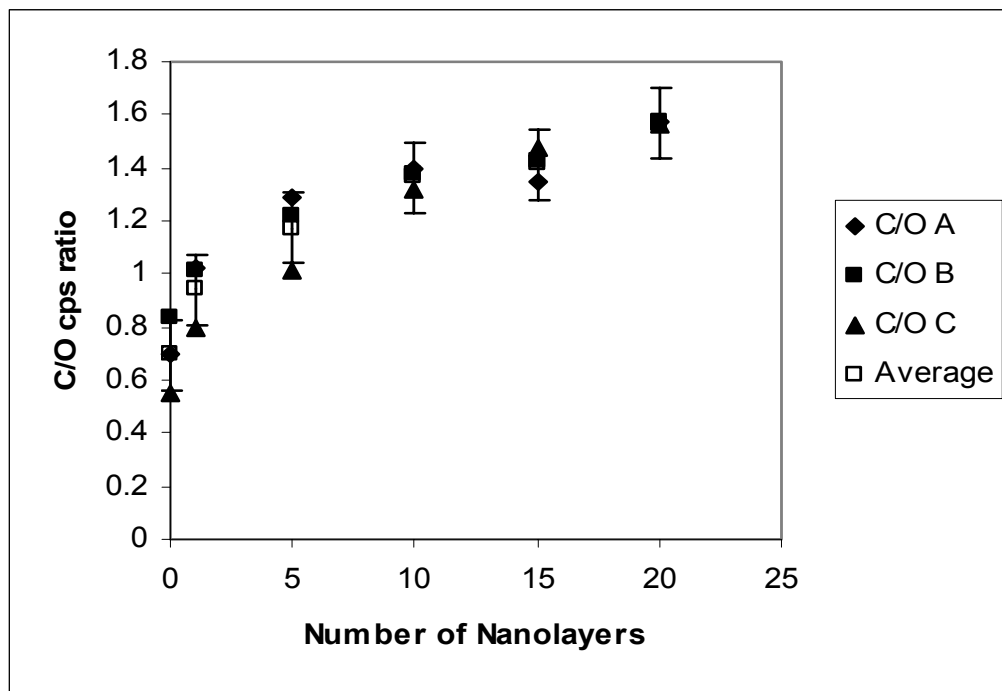


Figure 4-3. (1) Schematic of reflection path within FTIR-ATR device (2) Enhanced image of knit fabric structure showing gaps in the surface.

#### 4.1.2. Validation of the Substrate Charging Procedures

Due to the high surface heterogeneity of the cotton substrates, a thorough full factorial statistical analysis of the substrate preparation procedure was implemented. Three different formulations (Caustic:CR2000 mole ratios) were evaluated using nine specimens for a total of twenty seven experiments. The objective of these experiments was to determine the reproducibility of the technique as well as to quantify the effect of the caustic:CR2000 mole ratios on the electrostatic self-assembly deposition process.

Figure 4-4 illustrates the C/O cps ratio as a function of the number of deposited nanolayers for three different cationization procedures (A: 1.2, B: 1.55, C: 1.90). The average value of the C/O cps ratio as well as bars indicating the standard error are also presented in Figure 4-4.



**Figure 4-4. C/O cps ratio as a function of the number of deposited nanolayers for three different cationization procedures (A: 1.2, B: 1.55, C: 1.90).**

Based on the experimental results, it was observed that no statistical significant differences existed between the three cationization procedures. Figures 4-5 and 4-6 validate this assessment as they show a similar trend for the evolution of the N/O and S/O ratios as the number of nanolayers deposited increased. While the cationization mixture has been shown to influence the color and light fastness of dyes [59], it does not appear to affect the electrostatic self-assembly deposition of nanolayers. This behavior is in agreement with the nature of electrostatic self-assembly indicating that the deposition process is robust and can self-adapt to heterogeneous surfaces. In addition, the large number of anionic/cationic groups present in the polyelectrolytes contrast with the limited number of charged groups of the dyes allowing a better anchoring and depositing process.

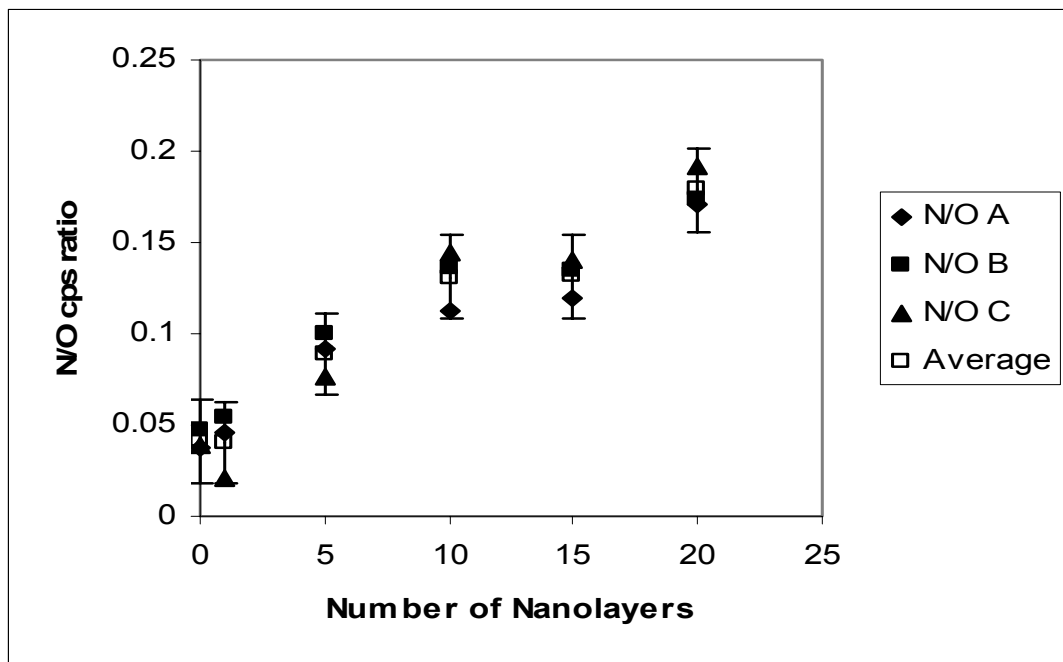


Figure 4-5. N/O cps ratio as a function of the number of deposited nanolayers for the three different cationization procedures (A: 1.2, B: 1.55, C: 1.90).

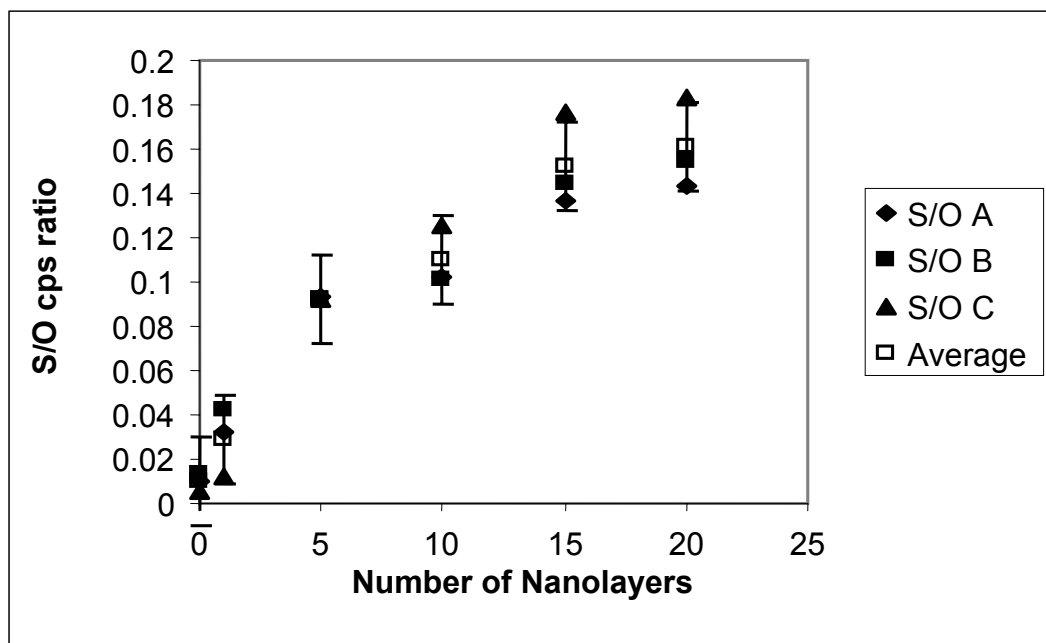
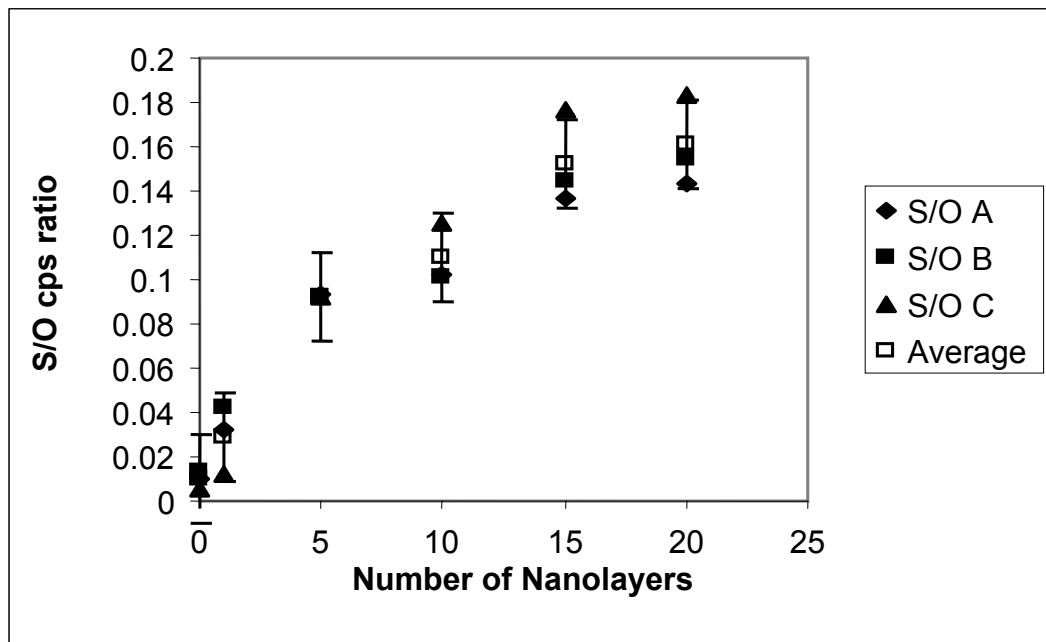


Figure 4-6. S/O cps ratio as a function of the number of deposited nanolayers for the three different cationization procedures (A: 1.2, B: 1.55, C: 1.90).

Determining the reproducibility of the deposition procedure was also important due to the use of a natural fiber as a substrate. Cationization procedure B, 1.55 ratio caustic:CR2000, was determined to be the one with the highest reproducibility. The experimental error was found to be less than 7% as shown in Figure 4-7.

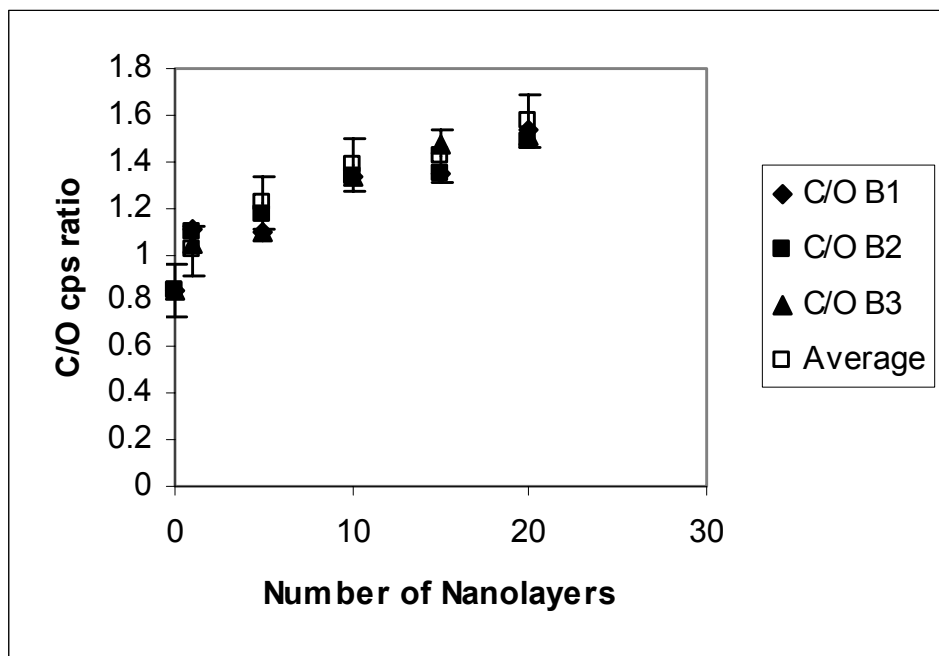


Figure 4-7. C/O cps ratio as a function of the number of deposited nanolayers for cationization procedure B (1.55 Caustic:CR2000 mole ratio).

### 4.1.3 XPS Measurements

X-ray photoelectron spectroscopy was used to examine the surfaces of the woven cotton fabrics as this technique was less sensitive to the porosity of the samples. Figure 4-8 illustrates a survey spectrum of an unmodified sample of woven cationic (1.55) cotton. As expected, there are large peaks at 281.91 eV and 528.91 eV indicating the presence of carbon and oxygen respectively. A trace amount of N (nitrogen) was also

detected at 398.91 eV. It is believed that the nitrogen is introduced into the surface of the cotton substrate by the cationic process. Figure 4-9 shows a survey spectrum of a 20-layer polyelectrolyte film supported on a woven cationic cotton substrate. PAH is the top layer on this sample. Peaks can be observed for both N and S (398.91 and 164.91 eV). The presence of N has been previously determined to be generated by the presence of PAH layers while the S has been reported to originate from the PSS layers. A comparison of Figures 4-8 and 4-9 indicates that XPS measurements can be used effectively to monitor the deposition process.



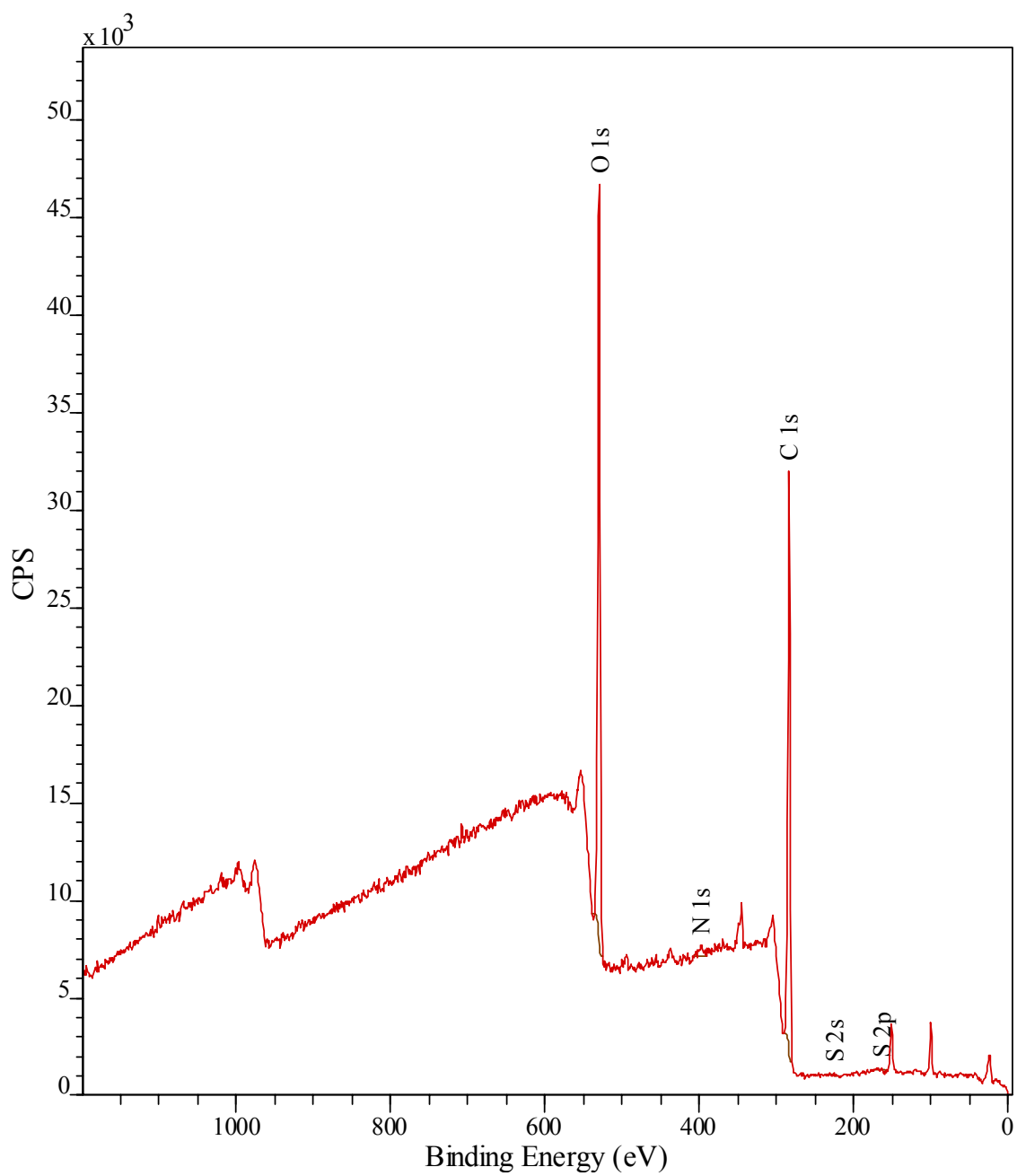


**Figure 4-8. XPS spectra for a cationically charged woven cotton fabric.**

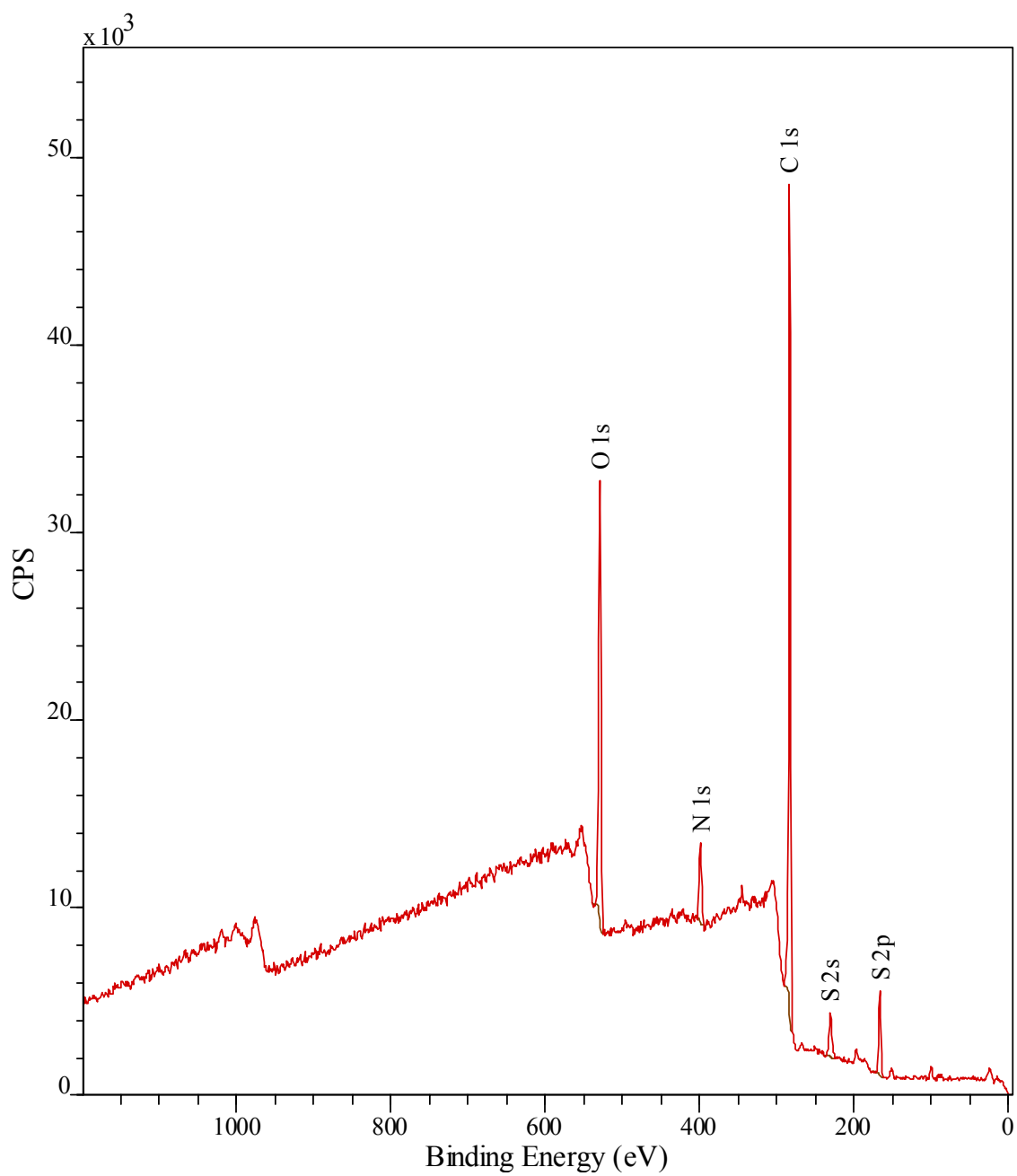


**Figure 4-9. XPS spectra for a cationically charged woven cotton fabric supporting 20 self-assembled layers with PAH being the top layer.**

Figure 4-10 illustrates the C/O cps ratios as a function of the number of deposited nanolayers. The increasing amount of C content as a function of the number of layers is evidence of the deposition process. Since the signal O is mainly originated by the hydroxyl groups in the surface of the cotton, the percent of oxygen is expected to decline as the number of layers deposited increase. An important feature not previously observed in planar substrates is the large initial increase in C/O ratio. This behavior may be explained on the basis of the porous nature of the cotton substrate. As the number of layers increase, the C/O ratio levels off as additional layers are deposited. This behavior is in agreement with previously published data and confirms that after a critical number of layers the deposition process is more dependent on the nature of the polyelectrolytes rather than that of the original substrate.

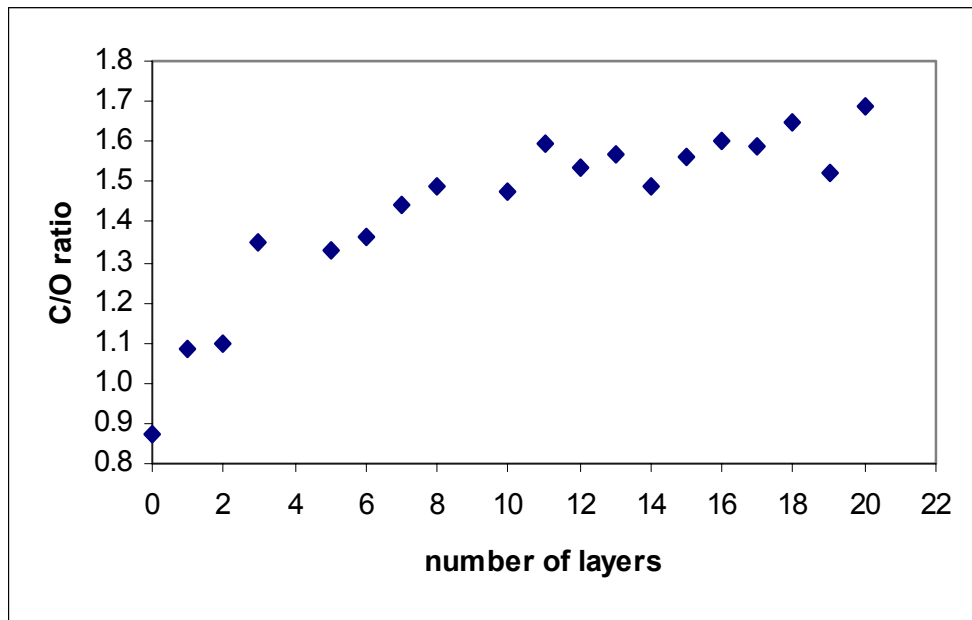


Figure 4-10. C/O ratio for woven cationic cotton samples coated with 20 self-assembled layers.

Figure 4-11 illustrates the evolution of the N/O cps ratio as a function of the number of deposited nanolayers. As previously reported by other research groups, the N signal mainly originates from the PAH layers.

A large variance is noted for the initial layers in a similar pattern as that exhibited by the C/O ratio of Figure 4-10. This behavior has not been previously reported when nanolayers of the same polyelectrolytes were deposited on controlled surfaces of silica and glass. The great variance exhibited during layers 1-5 can be explained on the basis of the high porosity and heterogeneity of the substrate. Initial layers face the intricate and tortuous pattern formed by the woven fibers. However, once a critical number of layers is deposited, the subsequent deposition process appeared to be unaffected by the nature of the substrate and exhibits a monotonical increase as previously reported in the literature for deposition on planar uniform surfaces.

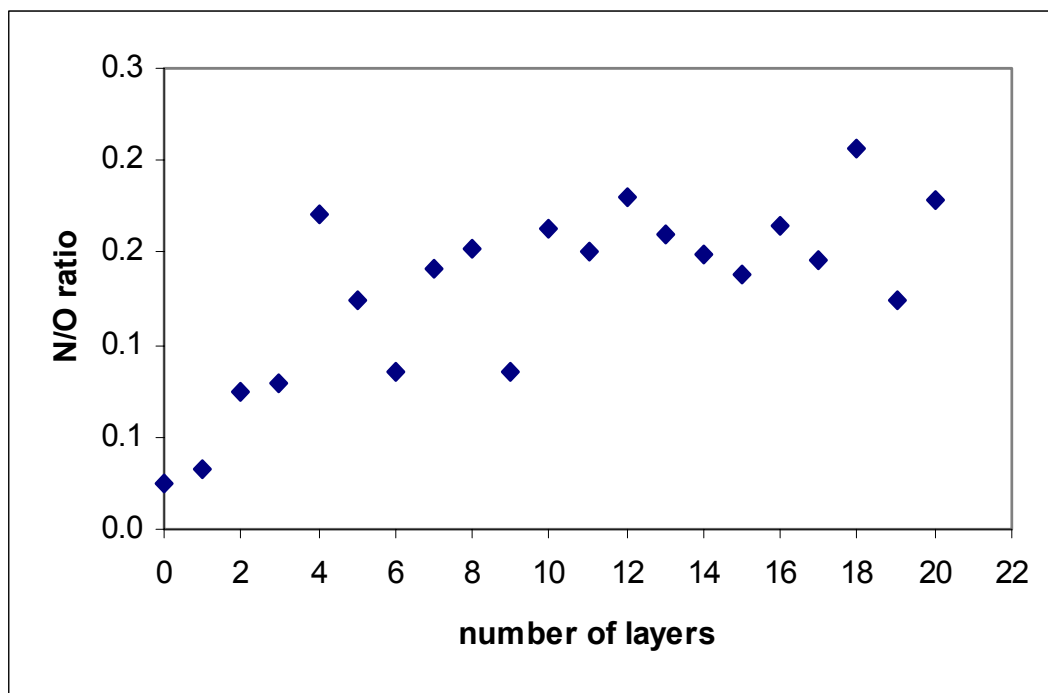


Figure 4-11. N/O ratio for woven cationic cotton samples with 20 self-assembled layers.

The evolution of the N/O ratio on the samples that contain PAH as the outermost layer is shown in Figure 4-12. That is to say: samples with an even number of deposited layers. An increasing trend in the N/O ratio is noted as the number of deposited layers increase. Again, large variations during the deposition of the initial layers support the hypothesis that the high porosity of the woven substrates appear to influence the efficiency of the deposition process. The relatively small initial value of the N/O ratio registers the presence of the cationic groups introduced by the chemical treatment of the cotton substrate.

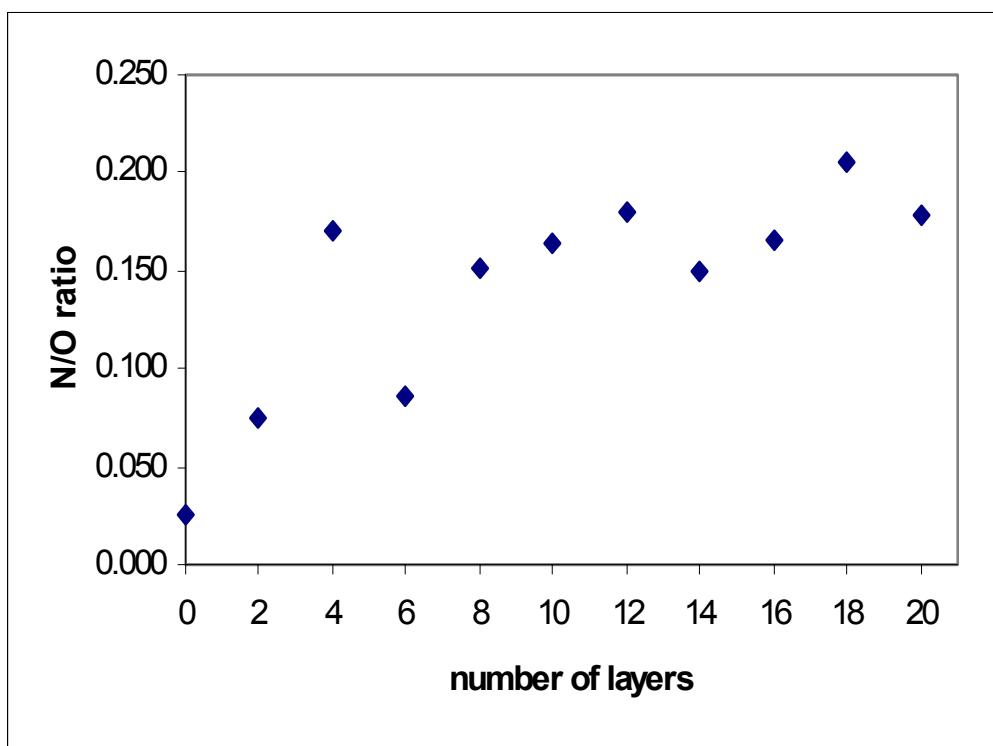


Figure 4-12. N/O ratio for woven cationic cotton samples containing a PAH layer on the top.

The increase in the ratio of S/O cps on the surface of the cotton sample as a result of the layer deposition process can be observed in Figure 4-13. As reported previously, the signal for S is generated by the layer containing PSS. The trend is very similar to that exhibited by the C/O and N/O ratios indicating the effective and alternate deposition of the layers. In a similar fashion, the initial behavior indicates high variation in the S/O ratio for the first layers deposited. This variation may be attributed to the high void percentage of the cotton substrate. Eventually, the S/O ratio gradually levels off as the number of layers deposited increases in agreement with previously published reports [

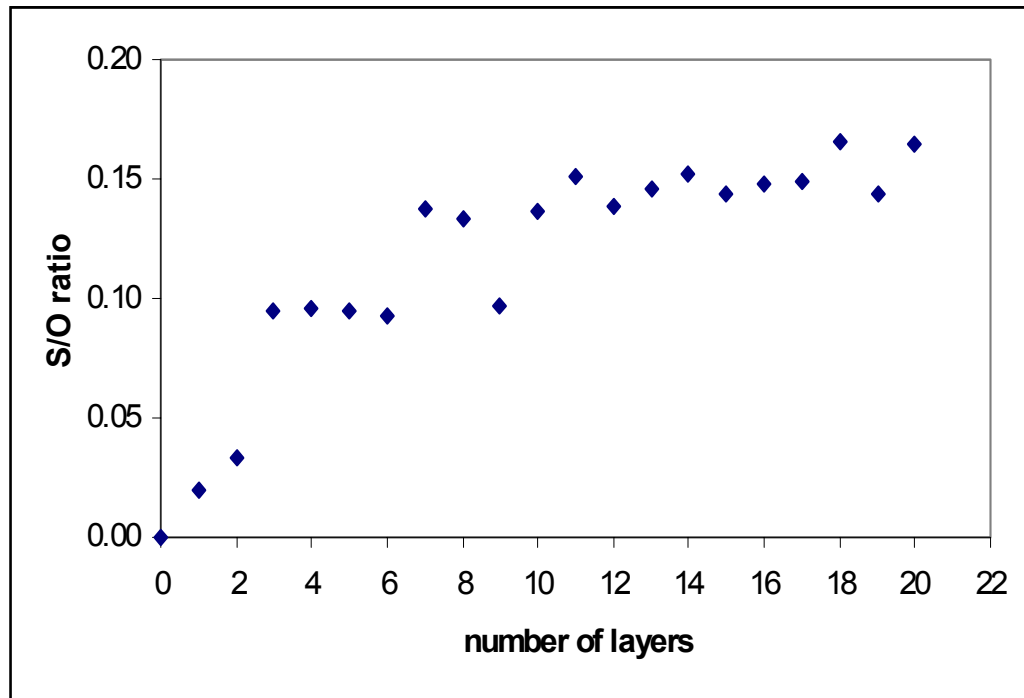
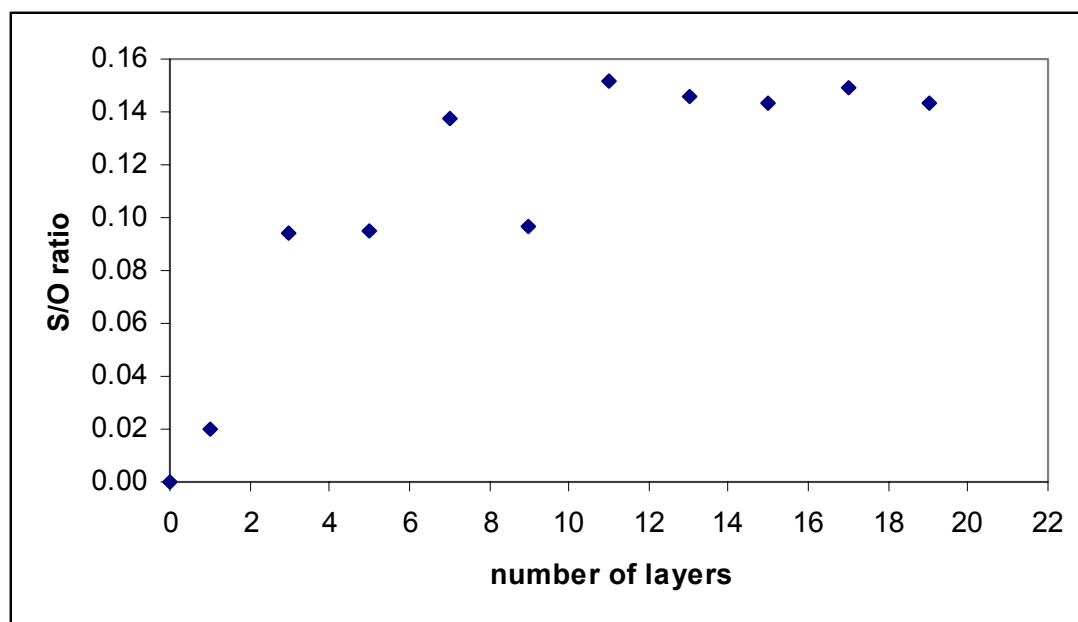


Figure 4-13. S/O ratio for woven cationic cotton fabrics coated with 20 self-assembled layers.

The evolution of the S/O ratio as a function of layer deposition for the samples that have PSS as the outermost layer is shown in Figure 4-14. An upward trend with large initial increases is again noted resembling the evolution of the C/O and N/O ratios as a function of layer deposition. The S/O ratio gradually levels off as a higher number of layers are deposited [8, 11, 132].



**Figure 4-14. S/O ratio for woven cationic cotton samples containing a PSS layer on top.**

In order to determine if the nanolayers were deposited over the cotton samples in a self-organized and stratified manner, a plot of the N/S ratios was generated from the XPS survey spectra. Figure 4-15 illustrates the evolution of the N/S ratio for 20 samples of cotton coated with alternated layers of PSS and PAH. The alternating behavior of the N/S as a function of number of layers clearly illustrates the stratification of the deposited layers. With the exception of the sixth and fourteenth points, all other points have alternating values. This behavior is due to the fact there is a higher N/S ratio for the films with PAH on top (even) than for those with PSS layer on top (odd). The values of points six and fourteen may be caused by the heterogeneity of the surface of the cotton substrate, film irregularity, or simply measurement error. As expected, Figure 4-15 exhibits again large amount of variance as the first layers are deposited onto the cotton



substrate followed by a more uniform progression. This trend is in agreement with the behavior of the C/O, N/O and S/O ratios shown in Figures 4-11 through 4-14.

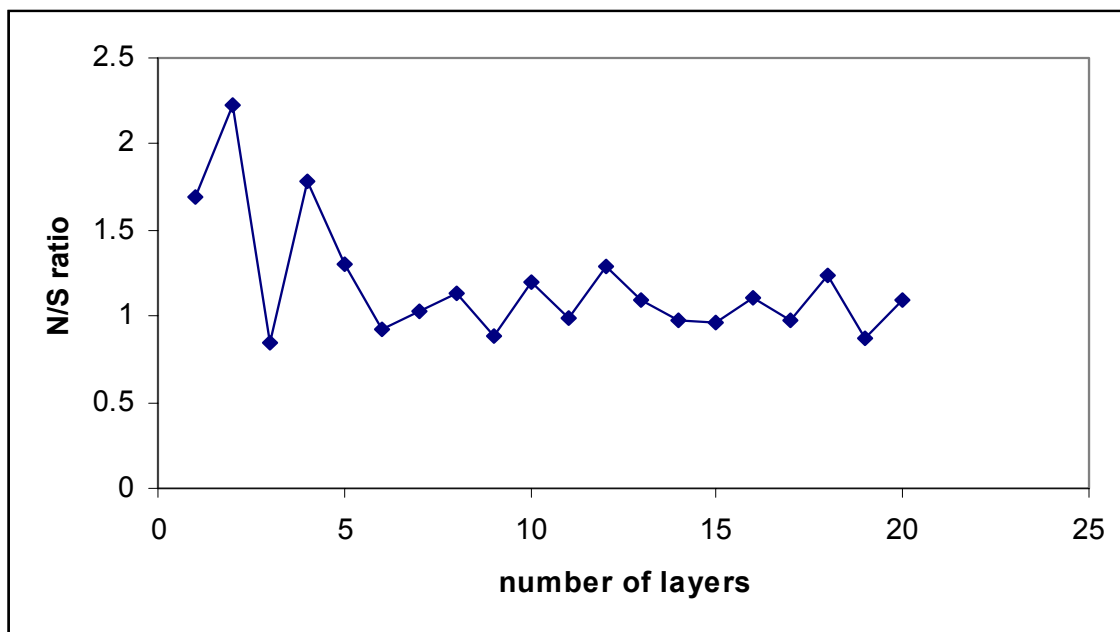


Figure 4-15. N/S ratio for woven cationic cotton supporting 20 alternating layers of PSS/PAH.

The XPS spectrum of cationically charged woven cotton fabric supporting 20 alternating layers of PSS and PAH is in quantitative agreement to spectra obtained in several previous studies involving layer-by-layer structures of PSS and PAH on several and different substrates. For example, Chen and McCarthy [11] reported the deposition of PSS and PAH onto poly(ethylene terephthalate) (PET) films. PAH ( $M_w = 50,000$ - $65,000$ ) and PSS ( $M_w = 70,000$ ) obtained from Aldrich were used. In their experimental procedure, the PET films were dipped in 0.02 M polyelectrolyte solution, removed after 20 min, rinsed with three aliquots of water, and then dipped in the oppositely charged polyelectrolyte solution. The samples were dried at room temperature at reduced

pressure before XPS analysis. XPS spectra were recorded on a Perkin-Elmer-Physical Electronics 5100 spectrometer with Al KR excitation (15 kV, 400 W). Spectra were taken and recorded at 15° and 75°, take-off angles. The 398.91 and 164.91 eV peaks were used to monitor N and S and determine the relative concentrations of PSS and PAH as well as the amount of stratification in the multilayers. Plots of N and S concentration as a function of the number of nanolayers correlate well with the data from the cotton samples. Both cotton and PET films exhibit an increase in the amount of N and S as the number of layers increases. The data reported for the PET exhibits a clear odd-even trend similar to that seen in the N/S ratio for the cotton sample. In addition, the amplitude of the odd-even trend was also seen to decrease with the addition of layers in agreement with the behavior of the cotton samples [11].

Furthermore, Levasalmi and McCarthy [132] analyzed the presence of layers of PSS and PAH on a poly(4-methyl-1-pentene) film. Solutions of the polyelectrolytes were prepared by dissolving 0.250 g of PAH and 0.750 g of PSS in 250 mL of water and adjusting pH to values ranging from 4-12. The samples were washed in water twice and once in water adjusted to the pH of the following deposition solution. After deposition, the samples were dried using a stream of nitrogen and then at reduced pressure overnight. XPS spectra for these films were obtained a takeoff angle 75° measured between the film surface plane and the entrance lens of the detector optics. XPS data gathered during this study correspond well with the data from the cotton samples. The S/O ratio for the PMPCOOH/PAH/PSS system is strikingly similar to the one of the cotton/PSS/PAH exhibiting large initial changes and then a leveling off as the number of layers increases.

The PMPCOOH multilayer assembly also presents an odd-even trend for the N/S ratio seen in the cotton samples. The N/S ratio for the PET film assembly was reported to be approximately 1.5 which compares well with the N/S ratio of 1.2 for the cotton multilayer assembly [132].

Phuvanartnuruks and McCarthy [8] used XPS as their principal analytical tool when analyzing multilayer structures of PSS and PAH on poly (chlorotrifluoroethylene) (PCTFE) films. Layer adsorptions were done at room temperature by the sequential dipping of the substrate into 0.02 M PAH and 0.02 M PSS solutions for twenty minutes. The samples were dried at room temperature under reduced pressure for 24 hours. XPS measurements were done at 15° and 75° take-off angles. The survey spectrum for the PCTFE multilayer assembly contains the same peaks of interest as the spectrum for the cotton multilayer assembly with peaks at N and S showing a monotonically increase in the values of N and S concentrations as the number of layers increases. The odd-even trend can again be seen in the N/S ratios for both the PCTFE and the cotton substrates. The amplitude of this trend decreases with the number of layers just as seen in the cotton multilayer assembly. A N/S ratio of approximately 1.2 for the PCTFE assembly was reported and it is very similar to the value of 1.2 reported in this study [8].

Delcorte and Bertrand [45] reported on the deposition of alternate polyelectrolyte coatings on various polymer substrates: poly(propylene), poly(isobutylene), poly(styrene), poly(methyl methacrylate), poly(ethylene terephthalate), poly(phenylene oxide), and poly(ether imide). The polyelectrolytes PSS and PAH were used to create the multilayer assemblies and were purchased from Aldrich. The concentration of the

solutions was 0.02 M. The samples were alternately dipped in the PSS and PAH with rinsing steps in between. The XPS equipment used in this study was a SSI-X-Probe (SSX-100/206 from Fisons)<sup>13</sup> with an aluminum anode (10 kV, 11.5 mA) and a quartz monochromator. A take-off angle of 35° with respect to the sample surface was used. In addition, XPS survey spectra of the different substrates used contained the same peaks as the cotton sample spectra with peaks at C, O, N, and S. The atomic concentrations of each of these elements were compared between untreated samples and samples supporting layers. All of the substrates showed increases in N and S as the number of layers deposited increased in a similar way as seen in the XPS data for the cotton multilayer assembly. Strikingly the values of the N/S equilibrate at 1.4, 1.2, 1.6, 1.3, 1.3 for PEI, PPO, PET, PMMA, PS respectively. These ratios are in quantitative agreement with the reported value of 1.2 for cotton substrates [45].

Other studies have demonstrated similar behavior of PSS and PAH assemblies on more homogenous substrates such as gold and silicon [18, 45]. For the silicon/PSS/PAH system a value of N/S ratio was reported to be 1.4, similar to the values reported for cotton.

#### **4.1.4 TEM Imaging**

Transmission electron microscopy was used to gather actual images of the multilayer thin films and to estimate the thickness of the polyelectrolyte layers. Figure 4-16 shows a low resolution TEM picture of a cotton fiber coated with 20 layers. The cuticle of the cotton fiber can be clearly seen on the right side of the image. The multilayer film can be seen to provide uniform conformal coating to the surface of the

fiber and it is estimated to be approximately of 325 nm in thickness. Upon close examination of the film, a high resolution image can be seen in Figure 4-17. The surface of the cotton fiber appears to be covered by a 19 nm thick film. Since the last layer deposited in this sample was PAH as confirmed by the XPS data, it is believed that the light gray area corresponds to PAH. The gradient in intensity in the upper side of the image is attributed to the curvature effects caused by the lobular shape of the cotton fiber. An additional picture taken at a resolution of 5 nm is shown in Figure 4-18 confirming the presence of a uniform coating with thickness varying from 18-22 nanometers.

The measurement of an individual nanolayer's thickness is recognized to not be an easy endeavor. Multi-angle XPS as well as ellipsometry have been extensively used on planar surfaces. However, due to the high curvature of the cotton substrates and the additional geometrical constrictions induced by the weaving process these techniques can not be used in this project. These images are believed to be the first ones to show direct evidence of the deposition on a high curvature substrate.

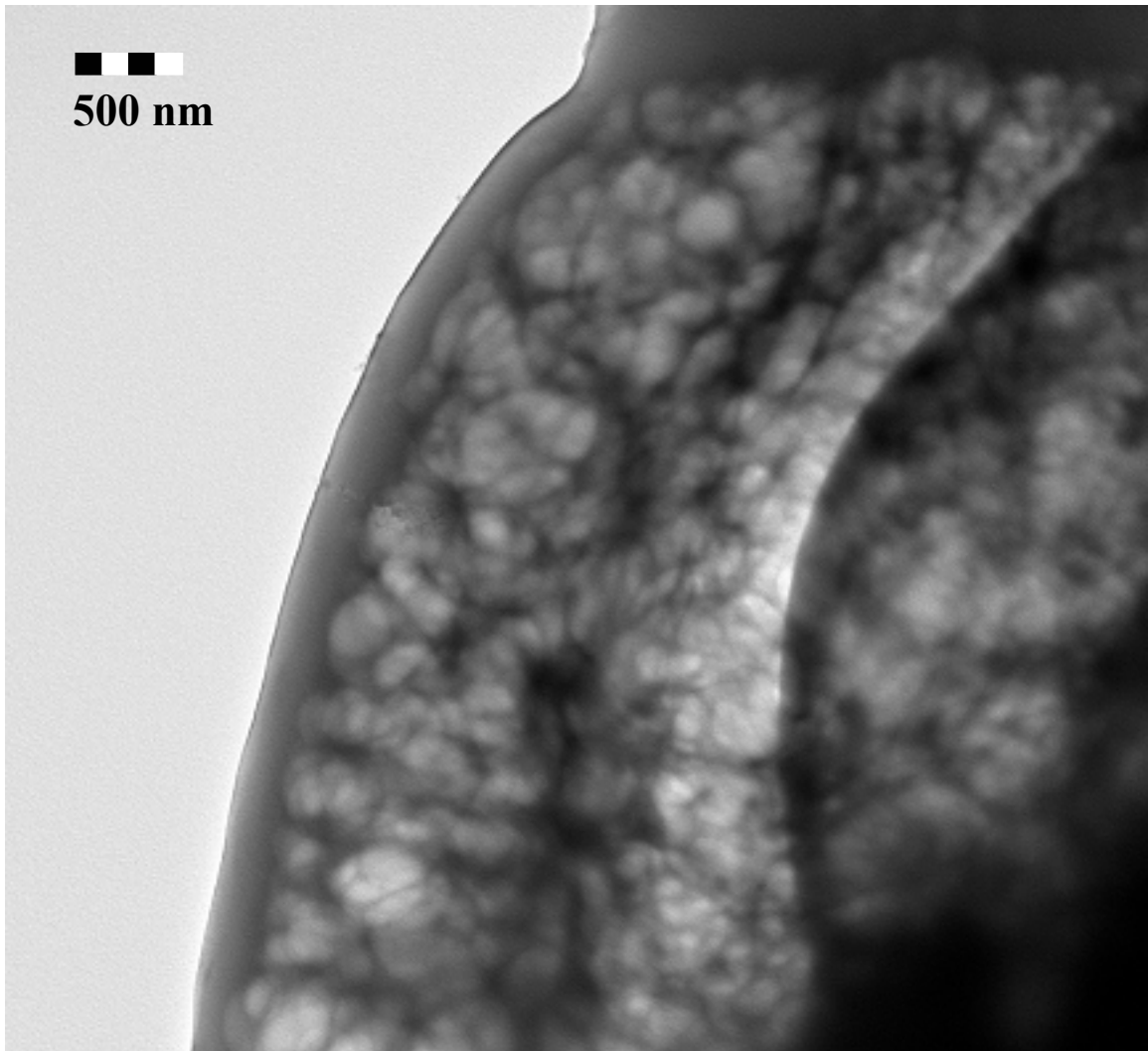


**Figure 4-16. TEM Image of a cotton fiber coated with a multilayer PSS/PAH film.**

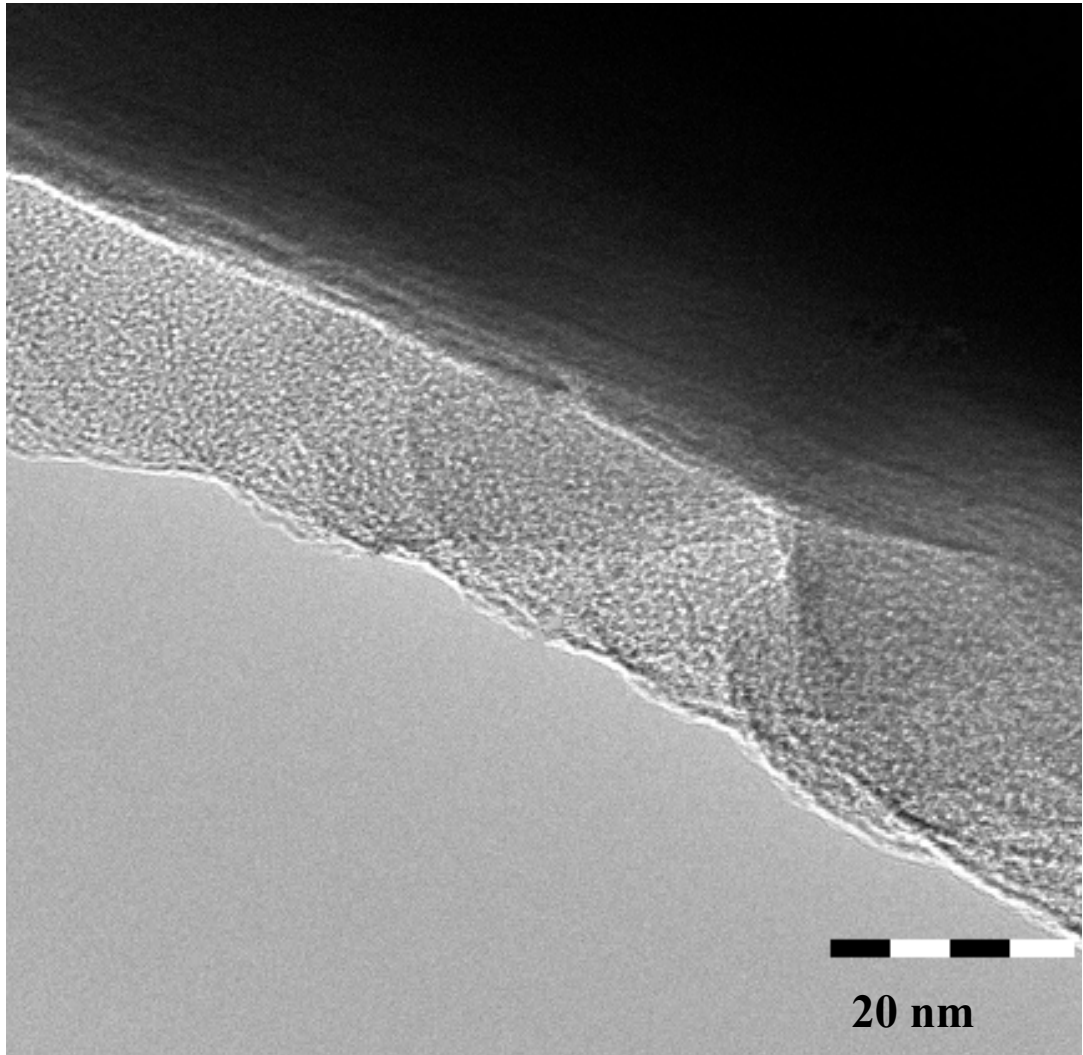


**Figure 4-17. TEM Image of a cotton fiber coated with a 20 layers of PSS/PAH .**

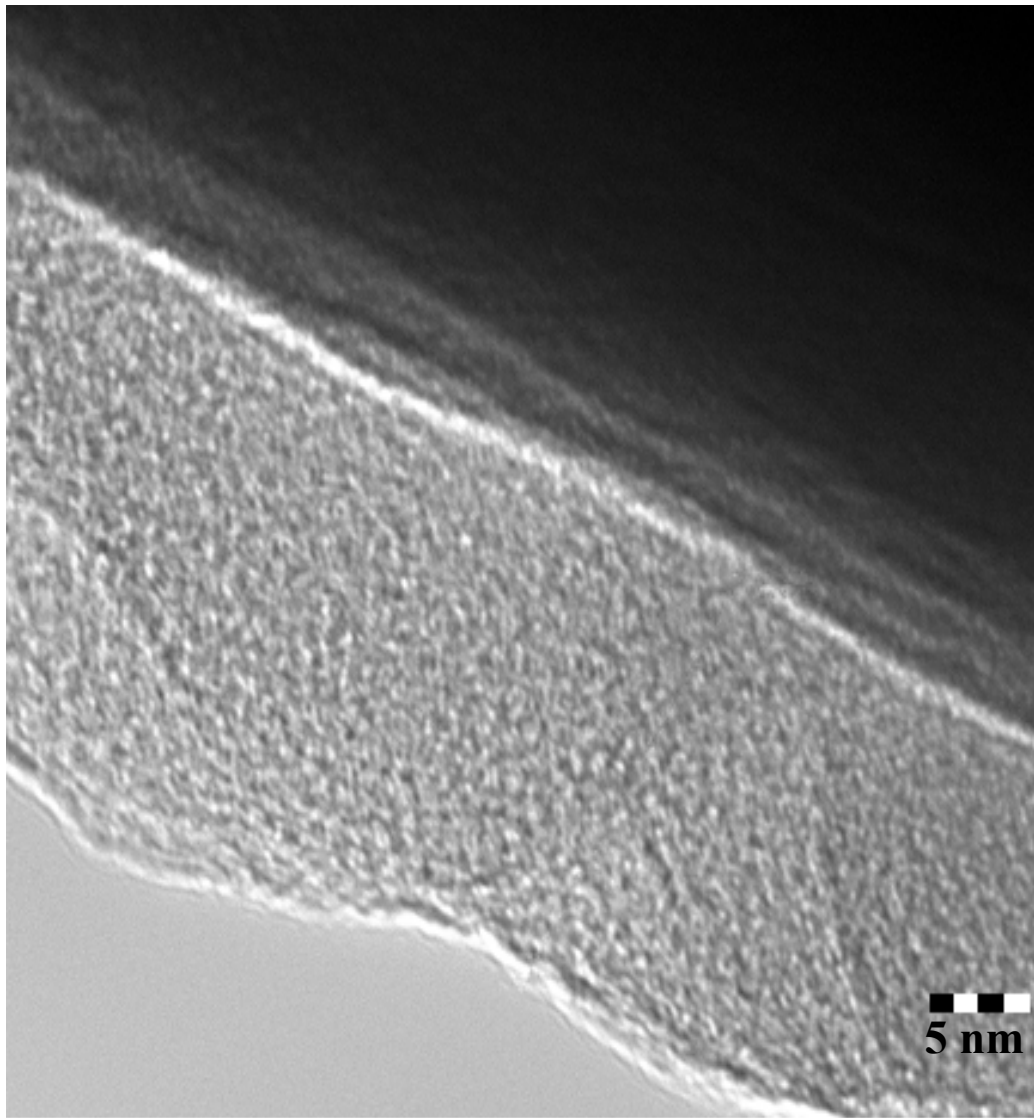


**Figure 4-18. High resolution TEM Image of a cationic cotton fiber coated with a 20 layers of PSS/PAH .**



### 4.1.5 PET Analysis

Samples of knit PET fabric plasma treated with 100 He were analyzed using XPS. Contact angle measurements were used to verify the application of the plasma treatment to the fabrics. Plasma treatment increased the hydrophilicity of the polyester, allowing the fabrics to be used as substrates for the electrostatic deposition of nanolayers. A survey spectrum of the plasma treated PET fabric with no polyelectrolyte layers can be seen in Figure 4-19. As expected, there are large peaks at 281.91 eV and 528.91 eV indicating the presence of carbon and oxygen respectively.

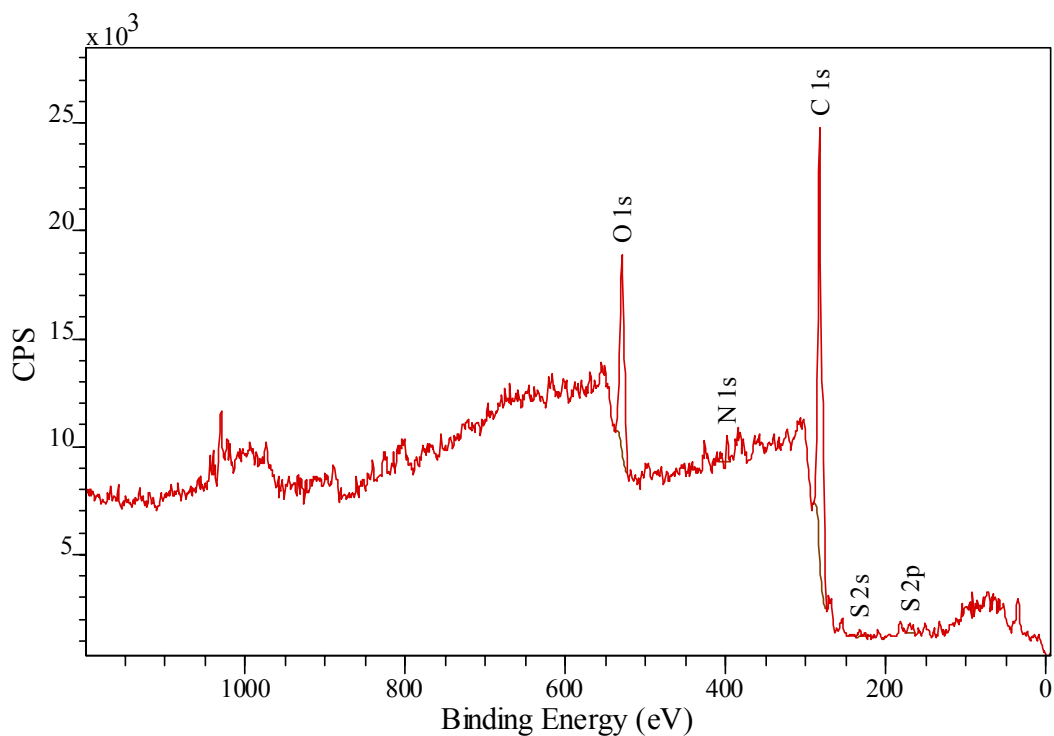


**Figure 4-19. XPS spectra for knit PET fabric plasma treated with 100 He.**

Figure 4-20 shows the XPS survey spectrum for a PET/PSS/PAH multilayer structure. Large peaks can now be seen for N at 398.91 eV and S at 164.91 eV. As

mentioned previously the presence of N has been determined to be generated by the presence of PAH layers while the S has been reported to originate from the PSS layers. Analysis of the N/S ratio, which can be seen in Figure 4-21, shows a similar trend to that seen for multilayer assemblies on cotton. Large initial variances can be seen but as the number of layers increases, the trend begins to level. The N/S ratio for the PET/PSS/PAH assembly is approximately 1.5, compared to 1.2 for the cotton sample. These spectra and data demonstrate that the electrostatic self-assembly process can be successfully applied to textile substrates that differ in material and structure.

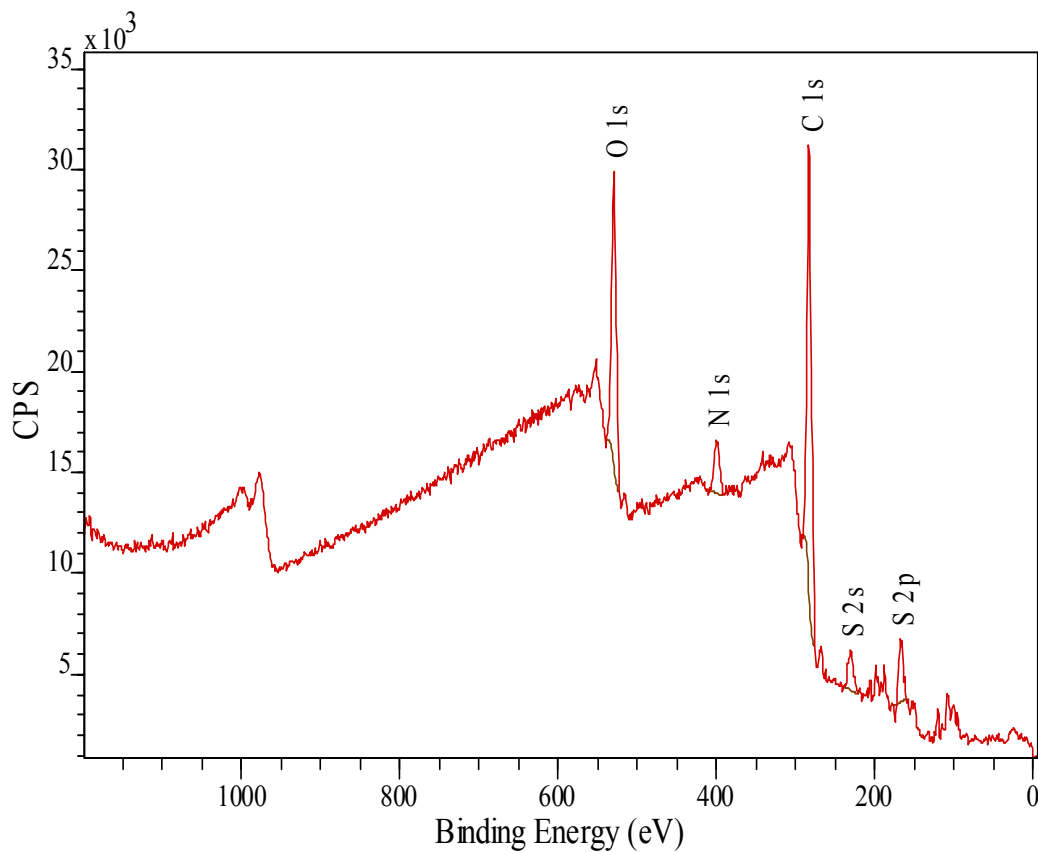


**Figure 4-20. XPS spectra for knit PET fabric plasma treated with 100 He supporting 20 self assembled layers.**

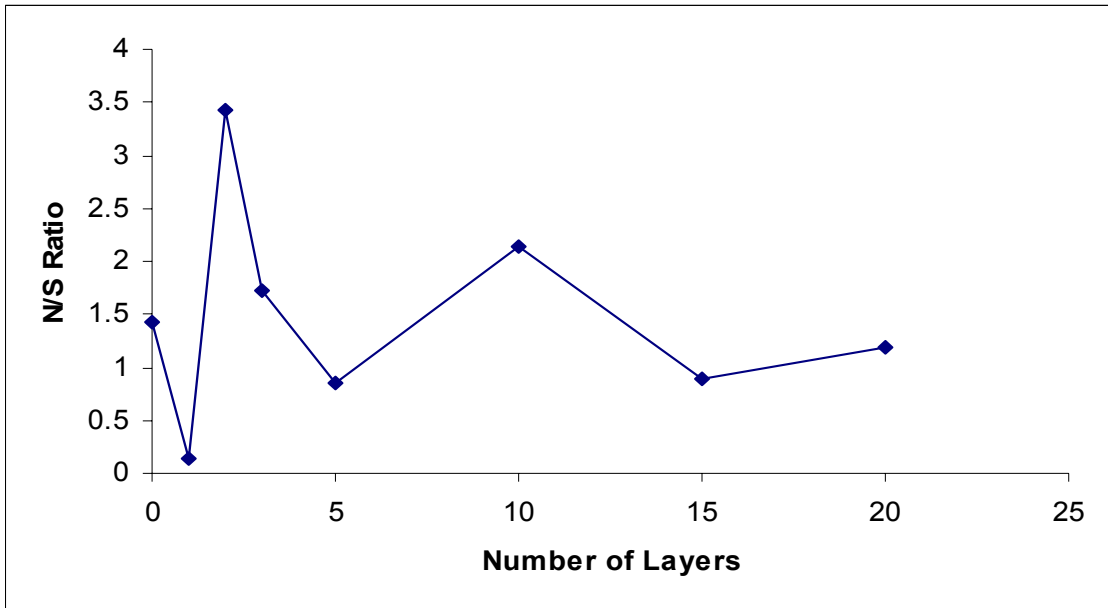


Figure 4-21. N/S ratio for plasma treated knit PET fabric supporting 20 alternating layers of PSS/PAH.

## CHAPTER 5: CONCLUSIONS

The electrostatic self-assembly deposition process was used to deposit alternate nanolayers of PSS and PAH on substrates of cotton and polyester fabric. Treatment of the cotton samples with 2,3-epoxypropyltrimethylammonium chloride was proven to be an effective procedure to create a substrate able to support multilayer thin films. XPS and TEM provided direct and indirect evidence of the efficacy of the deposition process. In addition, quantitative agreement of the XPS data with previously published data using several synthetic substrates corroborates that the layer-by-layer deposition process can be used a method for the modification of textile fibers and fabrics. This study also shows that electrostatic self-assembly is more dependent on the nature of the polyelectrolytes rather than that of the original substrate.

The experimental results of this research validate the feasibility of using the layer-by-layer deposition process to potentially develop functional textiles for protective clothing and selective filtration applications. Using nanolayer films as a method of textile modification will allow increases in the functionality of a variety of textile products. It is also possible that electrostatic self-assembly could be easily integrated into existing textile manufacturing processes.

## **CHAPTER 6: FUTURE WORK**

### **6.1 Future Substrates**

The successful completion of this research project provides the basic information needed to assemble multilayer thin films on a wide array of textile products. Any number of different textile fibers and fabrics could possibly be used as substrates for the electrostatic self-assembly of nanolayers. Fibers that can be treated in order to hold a surface charge can in theory be used as substrates for deposition. Possible candidates include nylon and wool fibers and fabrics. The substrates used for this research, cotton and polyester, should also be studied more in depth. Different types of both materials can be obtained and should be tested for their compatibility with the deposition process.

#### **6.1.1 Substrate Charging**

Further studies concerning the charging of textile substrates should also be conducted. The chemical solution used to charge the cotton for this research could be easily modified in order to determine the optimal settings that provide the highest level of surface charge on the cotton fibers. Changing the chemical solution and in turn the surface charge of the cellulose could affect many factors regarding the multilayer assembly. The deposition time, size of the layers, and uniformity of the layers could all be varied by changing the cationic charging process.

A large amount of work can be done in regards to the plasma treatment of polyester fabric. Changes can be made to the gases used, the gas mixtures, the dwell time in the plasma, the power level of the machine, and the value of the duty cycle. Studies

should also be made in an effort to determine why the plasma treatment of the samples is sometimes non-uniform.

## **6.2 Future Polyelectrolytes**

This research only looked at two polyelectrolyte systems. As mentioned previously, a number of different polyelectrolytes can be used to create multilayer thin films. Further experiments should be carried out that look at the effects of different polyelectrolytes on the performance of the modified textile. Certain polyelectrolytes could be used to provide anti-microbial, anti-soiling, or water repellent properties to the fibers or fabrics being treated.

## **6.3 Future Deposition Processes**

The deposition process used for this research was completely manual making the process extremely time consuming. Preparation of a sample with twenty layers of polyelectrolytes takes approximately 195 minutes. Also, since the process is done manually, it is susceptible to human error. If adequate attention is not given to the experimentation, mistakes will occur. At this time, some of the undergraduate students in Dr. Hinstroza's group are working on a way to automate the sample dipping process. This will be done using a mechanical system that will hold and dip the samples. Figure 6-1 shows a possible configuration of the automated system.

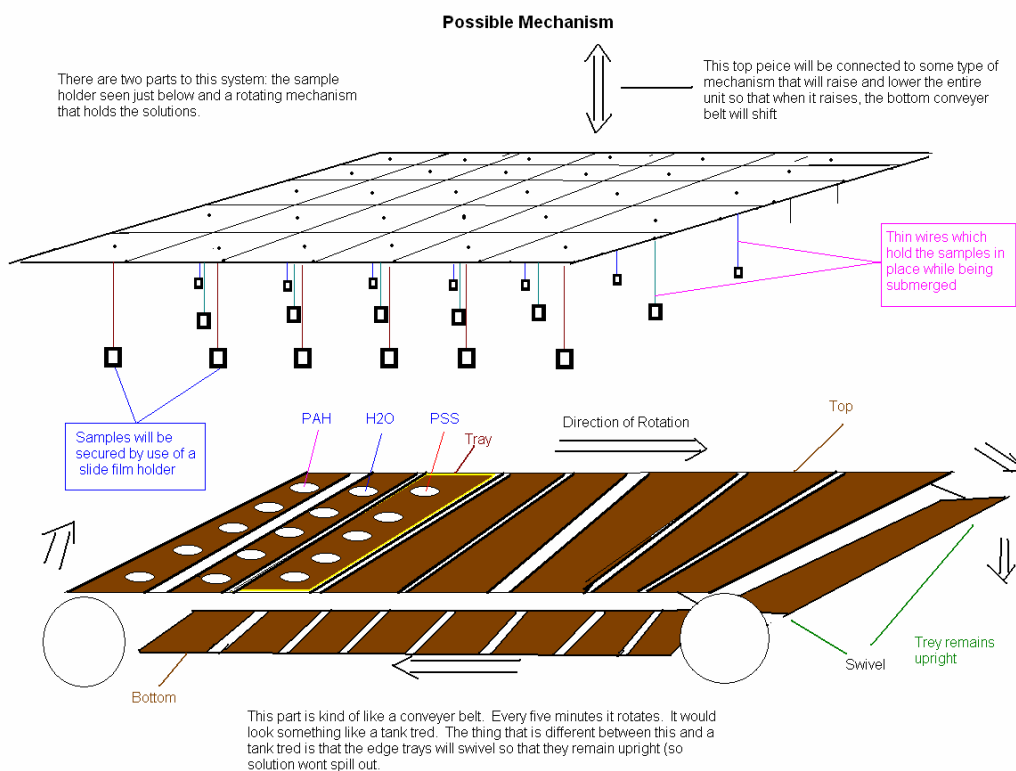


**Figure 6-1. Possible automated deposition system.**

## **6.4 Future Analysis Techniques**

Due to the nature of this research work as well as time constraints, it was not possible to use a large number of different analysis techniques. FTIR-ATR and XPS analysis were used due to the fact that they would be able to easily detect the nanoscale changes on the surface of the fabrics. These techniques do not require rigorous sample preparation and give good results in a relatively short amount of time. Now that it is clear that the fabrics are able support multilayer thin films, different analysis techniques can be used to clearly see what is happening on the surface of the fabric. Analysis

methods such as X-ray reflectance and quartz crystal microbalance can be used to look at the layers in detail and determine their thickness, uniformity, and stability.



## BIBLIOGRAPHY

1. Decher, G., *Fuzzy Nanoassemblies: Toward Layered Polymeric Multicomposites*. Science, 1997. **277**: p. 1232-1237.
2. Lvov, Y., G. Decher, and M. H., *Assembly, Structural Characterization, and Thermal Behavior of Layer-by-Layer Deposited Ultrathin Films of Poly(vinyl sulfite) and Poly(allylamine)*. Langmuir, 1993. **9**: p. 481-486.
3. Lvov, Y., G. Decher, and G. Sukhorukov, *Assembly of Thin Films by Means of Successive Deposition of Alternate Layers of DNA and Poly(allylamine)*. Macromolecules, 1993. **26**: p. 5396-5399.
4. Lvov, Y., F. Essler, and G. Decher, *Combination of Polycation/Polyanion Self-Assembly and Langmuir-Blodgett Transfer for the Construction of Superlattice Films*. J Phys Chem, 1993. **97**: p. 13773-13777.
5. Lvov, Y., et al., *Assembly of Polyelectrolyte Molecular Films onto Plasma-Treated Glass*. J Phys Chem, 1993. **97**: p. 12835-12841.
6. Bertrand, P., et al., *Ultrathin Polymer Coatings by Complexation of Polyelectrolytes at Interfaces: Suitable Materials, Structure, and Properties*. Macromol Rapid Commun, 2000. **21**: p. 319-348.
7. Hammond, P., *Recent Explorations in Electrostatic Multilayer Thin Film Assembly*. Curr Op Coll Inter Sci, 2000. **4**: p. 430-442.
8. Phuvanartnuruks, V. and T. McCarthy, *Stepwise Polymer Surface Modification: Chemistry-Layer-by-Layer Deposition*. Macromolecules, 1998. **31**: p. 1906-1914.
9. Tieke, B., et al., *Ultrathin Self-assembled Polyelectrolyte Multilayer Membranes*. Eur Phys J E, 2001. **5**: p. 29-39.
10. Ulman, A., *Formation and Structure of Self-Assembled Monolayers*. Chem Rev, 1996. **96**: p. 1533-1554.

11. Chen, W. and T. McCarthy, *Layer-by-Layer Deposition: A Tool for Polymer Surface Modification*. *Macromolecules*, 1997. **30**: p. 78-86.
12. Cooper, T.M., A.L. Campbell, and R.L. Crane, *Formation Of Polypeptide-Dye Multilayers By An Electrostatic Self-Assembly Technique*. *Langmuir*, 1995. **11**(7): p. 2713-2718.
13. Dubas, S. and J. Schlenoff, *Factors Controlling the Growth of Polyelectrolyte Multilayers*. *Macromolecules*, 1999. **32**: p. 8153-8160.
14. Hoogeveen, N.G., et al., *Formation and stability of multilayers of polyelectrolytes*. *Langmuir*, 1996. **12**(15): p. 3675-3681.
15. Losche, M., et al., *Detailed Structure of Molecularly Thin Polyelectrolyte Multilayer Films on Solid Substrates as Revealed by Neutron Reflectometry*. *Macromolecules*, 1998. **31**: p. 8893-8906.
16. Schmitt, J., et al., *Internal Structure of Layer-by-Layer Adsorbed Polyelectrolyte Films: A Neutron and X-ray Reflectivity Study*. *Macromolecules*, 1993(26): p. 7058-7063.
17. Decher, G., *Polyelectrolyte Multilayers, an Overview*, G. Decher and J. Schlenoff, Editors. 2003, Wiley-VCH. p. 1-46.
18. Caruso, F., et al., *Ultrathin Multilayer Polyelectrolyte Films on Gold: Construction and Thickness Determination*. *Langmuir*, 1997. **13**: p. 3422-3426.
19. Yoo, D., S. Shiratori, and M. Rubner, *Controlling Bilayer Composition and Surface Wettability of Sequentially Adsorbed Multilayers of Weak Polyelectrolytes*. *Macromolecules*, 1998. **31**: p. 4309-4318.
20. Feldheim, D.L., et al., *Electron Transfer in Self-Assembled Inorganic Polyelectrolyte/Metal Nanoparticle Heterostructures*. *Journal of the American Chemical Society*, 1996(118): p. 7640-7641.
21. Keller, S.W., H. Kim, and T.E. Mallouk, *Layer-by-Layer Assembly of Intercalation Compounds and Heterostructures on Surfaces: Toward Molecular*

- "Beaker" Epitaxy. Journal of the American Chemical Society, 1994(116): p. 8817-8818.
22. Lvov, Y., et al., *Assembly of Multicomponent Protein Films by Means of Electrostatic Layer-by-Layer Adsorption*. Journal of the American Chemical Society, 1995(117): p. 6117-6123.
  23. Lvov, Y., et al., *Formation of ultrathin multilayer and hydrated gel from montmorillonite and linear polycations*. Langmuir, 1996. **12**(12): p. 3038-3044.
  24. Lvov, Y., et al., *A Careful Examination of the Adsorption Step in the Alternate Layer-by-Layer Assembly of Linear Polyanion and Polycation*. Coll Surf A, 1999. **146**: p. 337-346.
  25. Delcorte, A., et al., *ToF-SIMS Study of Alternate Polyelectrolyte Thin Films: Chemical Surface Characterization and Molecular Secondary Ions Sampling Depth*. Surface Science, 1996. **366**: p. 149-165.
  26. Fogden, A. and B.W. Ninham, *Electrostatics of curved fluid membranes: The interplay of direct interactions and fluctuations in charged lamellar phases*. Adv Coll Int Sci, 1999. **83**: p. 85-110.
  27. Ninham, B.W., K. Kurihara, and O.I. Vinogradova, *Hydrophobicity, Specific Ion Adsorption and Reactivity*. Coll Surf A, 1997. **123-124**: p. 7-12.
  28. Kotov, N., *Layer-by-Layer Self-Assembly: The Contribution of Hydrophobic Interactions*. Nanostruc Mat, 1999. **12**: p. 789-796.
  29. Advincula, R., E. Fells, and M. Park, *Molecularly Ordered Low Molecular Weight Azobenzene Dyes and Polycation Alternate Multilayer Films: Aggregation, Layer Order, and Photoalignment*. Chem Mater, 2001. **13**: p. 2870-2878.
  30. Decher, G., Y. Lvov, and J. Schmitt, *Proof of Multilayer Structural Organization in Self-assembled Polycation-Polyanion Molecular Films*. Thin Solid Films, 1994. **244**: p. 772-777.

31. Fendler, J., *Preparation and Utilization of Self-assembled Ultrathin Films Composed of Polyelectrolytes, Nanoparticles and Nanoplatelets*. CCACAA, 1998. **71**: p. 1127-1137.
32. Kato, N., et al., *Thin Multilayer Films of Weak Polyelectrolytes on Colloid Particles*. *Macromolecules*, 2002. **35**: p. 9780-9787.
33. Advincula, R., *Supramolecular Strategies Using the Layer-by-Layer Sequential Assembly Technique: Applications for PLED and LC Display Devices and Biosensors*. *IEICE Trans Electron*, 2000. **E83-C**: p. 1104-1111.
34. Advincula, R., et al., *Photo-induced Alignment of Polymer Ultrathin Films Fabricated by Alternate Self-assembly Solution Adsorption of Polyelectrolytes and Small Azo Dye Chromophores*. *ACS Polymer Preprints*, 1999. **Spring**: p. 1-2.
35. Lvov, Y., et al., *Thin Film Nanofabrication via Layer-by-Layer Adsorption of Tubule Halloysite, Spherical Silica, Proteins, and Polycations*. *Coll Surf A*, 2002. **198-200**: p. 375-382.
36. Kleinfield, E. and G. Ferguson, *Healing of Defects in the Stepwise Formation of Polymer/Silicate Multilayer Films*. *Chem Mater*, 1996. **8**: p. 1575-1578.
37. Cassagneau, T. and J. Fendler, *Preparation and Layer-by-Layer Self-Assembly of Silver Nanoparticles Capped by Graphite Oxide Nanosheets*. *J Phys Chem B*, 1999. **103**: p. 1789-1793.
38. Artyukhin, A.B., et al., *Layer-by-layer electrostatic self-assembly of polyelectrolyte nanoshells on individual carbon nanotube templates*. *Langmuir*, 2004. **20**(4): p. 1442-1448.
39. Caruso, F., et al., *Quartz Crystal Microbalance and Surface Plasmon Resonance Study of Surfactant Adsorption onto Gold and Chromium Oxide Surfaces*. *Langmuir*, 1995. **11**: p. 1546-1552.
40. Lu, C.H., et al., *Au nanoparticle micropatterns prepared from self-assembled films*. *Langmuir*, 2004. **20**(3): p. 974-977.

41. GirardEgrot, A.P., R.M. Morelis, and P.R. Coulet, *Direct influence of the interaction between the first layer and a hydrophilic substrate on the transition from Y- to Z-type transfer during deposition of phospholipid Langmuir-Blodgett films*. Langmuir, 1996. **12**(3): p. 778-783.
42. Watanabe, S. and S.L. Regen, *Dendrimers As Building-Blocks For Multilayer Construction*. Journal Of The American Chemical Society, 1994. **116**(19): p. 8855-8856.
43. Tronin, A., Y. Lvov, and C. Nicolini, *Ellipsometry And X-Ray Reflectometry Characterization Of Self-Assembly Process Of Polystyrenesulfonate And Polyallylamine*. Colloid And Polymer Science, 1994. **272**(10): p. 1317-1321.
44. Sano, M., Y. Lvov, and T. Kunitake, *Formation of Ultrathin Polymer Layers on Solid Substrates by Means of Polymerization-induced Epitaxy and Alternate Adsorption*. Ann Rev Mat Sci, 1996. **26**: p. 153-187.
45. Delcorte, A., et al., *Adsorption of polyelectrolyte multilayers on polymer surfaces*. Langmuir, 1997. **13**(19): p. 5125-5136.
46. Lutt, M., M.R. Fitzsimmons, and D. Li, *X-ray Reflectivity Study of Self-Assembled Thin Films of Macrocycles and Macromolecules*. Journal of Physical Chemistry B, 1998(102): p. 400-405.
47. Bergbreiter, D.E., J.G. Franchina, and K. Kabza, *Hyperbranched grafting on oxidized polyethylene surfaces*. Macromolecules, 1999. **32**(15): p. 4993-4998.
48. Schlenoff, J.B., H. Ly, and M. Li, *Charge and mass balance in polyelectrolyte multilayers*. Journal Of The American Chemical Society, 1998. **120**(30): p. 7626-7634.
49. Ferreira, M., J.H. Cheung, and M.F. Rubner, *Molecular Self-Assembly Of Conjugated Polyions - A New Process For Fabricating Multilayer Thin-Film Heterostructures*. Thin Solid Films, 1994. **244**(1-2): p. 806-809.

50. Decher, G., et al., *New Nanocomposite Films For Biosensors - Layer-By-Layer Adsorbed Films Of Polyelectrolytes, Proteins Or Dna*. *Biosensors & Bioelectronics*, 1994. **9**(9-10): p. 677-684.
51. Fou, A.C. and M. Rubner, *Molecular-Level Processing of Conjugated Polymers. 2. Layer-by-Layer Manipulation of In-Situ Polymerized p - m e Doped Conducting Polymers*. *Macromolecules*, 1995(28): p. 7115-7120.
52. Brynda, E. and M. Houska, *Multiple alternating molecular layers of albumin and heparin on solid surfaces*. *Journal Of Colloid And Interface Science*, 1996. **183**(1): p. 18-25.
53. Godinez, L.A., et al., *Multilayer self-assembly of amphiphilic cyclodextrin hosts on bare and modified gold substrates: Controlling aggregation via surface modification*. *Langmuir*, 1998. **14**(1): p. 137-144.
54. Riccardi, C., et al., *Surface Modification of Poly(ethylene terephthalate) Fibers Induced by Radio Frequency Air Plasma Treatment*. *Applied Surface Science*, 2003. **211**: p. 386-397.
55. Hammond, P.T. and G.M. Whitesides, *Formation Of Polymer Microstructures By Selective Deposition Of Polyion Multilayers Using Patterned Self-Assembled Monolayers As A Template*. *Macromolecules*, 1995. **28**(22): p. 7569-7571.
56. Advincula, R. and W. Knoll, *Supramolecular thin films via the Langmuir-Blodgett-Kuhn (LBK) technique*. *Colloids And Surfaces A-Physicochemical And Engineering Aspects*, 1997. **123**: p. 443-455.
57. Advincula, R., et al., *In situ investigations of polymer self-assembly solution adsorption by surface plasmon spectroscopy*. *Langmuir*, 1996. **12**(15): p. 3536-3540.
58. Gao, M.Y., et al., *Constructing Pbi<sub>2</sub> Nanoparticles Into A Multilayer Structure Using The Molecular Deposition (Md) Method*. *Journal Of The Chemical Society- Chemical Communications*, 1994(24): p. 2777-2778.

59. Hauser, P.J. and A.R. Tappa, *Improving the environmental and economic aspects of cotton dyeing using a cationised cotton*. *Coloration Technology*, 2001(117): p. 282-288.
60. Linford, M.R., M. Auch, and H. Mohwald, *Nonmonotonic Effect of Ionic Strength on Surface Dye Extraction during Dye-Polyelectrolyte Multilayer Formation*. *Journal of American Chemical Society*, 1998(120): p. 178-182.
61. Ariga, K., Y. Lvov, and T. Kunitake, *Assembling Alternate Dye-Polyion Molecular Films by Electrostatic Layer-by-Layer Adsorption*. *Journal of American Chemical Society*, 1997(119): p. 2224-2231.
62. Li, D., et al., *Preparation, Characterization, and Properties of Mixed Organic and Polymeric Self-Assembled Multilayers*. *Journal of American Chemical Society*, 1998(120): p. 8797-8804.
63. Kurth, D.G. and R. Osterhout, *In Situ Analysis of Metallosupramolecular Coordination Polyelectrolyte Films by Surface Plasmon Resonance Spectroscopy*. *Langmuir*, 1999(15): p. 4842-4846.
64. Kolarik, L., et al., *Building Assemblies from High Molecular Weight Polyelectrolytes*. *Langmuir*, 1999(15): p. 8265-8275.
65. Cochlin, D., et al., *Layered Nanostructures with LC-Polymers, Polyelectrolytes, and Inorganics*. *Macromolecules*, 1997(30): p. 4775-4779.
66. Onda, M., et al., *Sequential actions of glucose oxidase and peroxidase in molecular films assembled by layer-by-layer alternate adsorption*. *Biotechnology And Bioengineering*, 1996. **51**(2): p. 163-167.
67. Onitsuka, O., et al., *Enhancement of light emitting diodes based on self-assembled heterostructures of poly(p-phenylene vinylene)*. *Journal Of Applied Physics*, 1996. **80**(7): p. 4067-4071.
68. Wu, A., et al., *Solid-state light-emitting devices based on the tris-chelated ruthenium(II) complex: 3. High efficiency devices via a layer-by-layer molecular-*

- level blending approach*. Journal Of The American Chemical Society, 1999. **121**(20): p. 4883-4891.
69. Arys, X., et al., *Ordered polyelectrolyte multilayers. Rules governing layering in organic binary multilayers*. Journal Of The American Chemical Society, 2003. **125**(7): p. 1859-1865.
  70. Arys, X., A. Laschewsky, and A.M. Jonas, *Ordered polyelectrolyte "multilayers". I. Mechanisms of growth and structure formation: A comparison with classical fuzzy "multilayers"*. Macromolecules, 2001. **34**(10): p. 3318-3330.
  71. Cho, J. and K. Char, *Effect of layer integrity of spin self-assembled multilayer films on surface Wettability*. Langmuir, 2004. **20**(10): p. 4011-4016.
  72. Dhanabalan, A., et al., *A study of Langmuir and Langmuir-Blodgett films of polyaniline*. Langmuir, 1997. **13**(16): p. 4395-4400.
  73. Facchetti, A., et al., *Design and preparation of zwitterionic organic thin films: self-assembled siloxane-based, thiophene-spaced N-benzylpyridinium dicyanomethanides as nonlinear optical materials*. Langmuir, 2001. **17**(19): p. 5939-5942.
  74. Hillebrandt, H., et al., *High electric resistance polymer/lipid composite films on indium-tin-oxide electrodes*. Langmuir, 1999. **15**(24): p. 8451-8459.
  75. Joly, S., et al., *Multilayer nanoreactors for metallic and semiconducting particles*. Langmuir, 2000. **16**(3): p. 1354-1359.
  76. Liang, Z.Q. and Q. Wang, *Multilayer assembly and patterning of poly(p-phenylenevinylene)s via covalent coupling reactions*. Langmuir, 2004. **20**(22): p. 9600-9606.
  77. Park, M.K., et al., *Self-assembly and characterization of polyaniline and sulfonated polystyrene multilayer-coated colloidal particles and hollow shells*. Langmuir, 2003. **19**(20): p. 8550-8554.



78. Ram, M.K., et al., *Physical properties of polyaniline films: Assembled by the layer-by-layer technique*. Langmuir, 1999. **15**(4): p. 1252-1259.
79. Raposo, M. and O.N. Oliveira, *Adsorption of poly(o-methoxyaniline) in layer-by-layer films*. Langmuir, 2002. **18**(18): p. 6866-6874.
80. Wu, D.G., et al., *Photosensitized electron injection from an ITO electrode to trichromophore dyes deposited on Langmuir-Blodgett films*. Langmuir, 1999. **15**(21): p. 7276-7281.
81. Yuan, C.W., et al., *Insertion Of Polypyrrole Into Arachidic Acid Langmuir-Blodgett-Films*. Langmuir, 1995. **11**(1): p. 5-7.
82. Koetse, M., et al., *Ultrathin coatings by multiple polyelectrolyte adsorption/surface activation (CoMPAS)*. Macromolecules, 1998. **31**(26): p. 9316-9327.
83. Wu, A.P., J. Lee, and M.F. Rubner, *Light emitting electrochemical devices from sequentially adsorbed multilayers of a polymeric ruthenium (II) complex and various polyanions*. Thin Solid Films, 1998. **329**: p. 663-667.
84. Arys, X., et al., *Ultrathin multilayers made by alternate deposition of ionenes and polyvinylsulfate: from unstable to stable growth*. Thin Solid Films, 1998. **329**: p. 734-738.
85. Arys, X., et al., *Structural studies on thin organic coatings built by repeated adsorption of polyelectrolytes*. Progress In Organic Coatings, 1998. **34**(1-4): p. 108-118.
86. Lee, J.K., D. Yoo, and M.F. Rubner, *Synthesis and characterization of an electroluminescent polyester containing the Ru(II) complex*. Chemistry Of Materials, 1997. **9**(8): p. 1710-&.
87. Hodak, J., et al., *Layer-by-layer self-assembly of glucose oxidase with a poly(allylamine)ferrocene redox mediator*. Langmuir, 1997. **13**(10): p. 2708-2716.

88. Yoo, D., et al., *New electro-active self-assembled multilayer thin films based on alternately adsorbed layers of polyelectrolytes and functional dye molecules*. Synthetic Metals, 1997. **85**(1-3): p. 1425-1426.
89. Ninham, B.W. and V. Yaminsky, *Ion binding and ion specificity: The Hofmeister effect and Onsager and Lifshitz theories*. Langmuir, 1997. **13**(7): p. 2097-2108.
90. Keller, S.W., et al., *Photoinduced charge separation in multilayer thin films grown by sequential adsorption of polyelectrolytes*. Journal Of The American Chemical Society, 1995. **117**(51): p. 12879-12880.
91. Keller, S.W., et al., *Photochemically And Electrochemically Driven Charge-Transport In Lamellar Redox Polymer Arrays*. Abstracts Of Papers Of The American Chemical Society, 1995. **210**: p. 83-COLL.
92. Anzai, J., et al., *Layer-by-layer construction of multilayer thin films composed of avidin and biotin-labeled poly(amine)s*. Langmuir, 1999. **15**(1): p. 221-226.
93. Laschewsky, A., et al., *Molecular recognition by hydrogen bonding in polyelectrolyte multilayers*. Chemistry-A European Journal, 1997. **3**(1): p. 34-38.
94. Decher, G., et al., *Layer-By-Layer Adsorbed Films Of Polyelectrolytes, Proteins Or Dna*. Abstracts Of Papers Of The American Chemical Society, 1993. **205**: p. 334-POLY.
95. Caruso, F., et al., *Magnetic core-shell particles: Preparation of magnetite multilayers on polymer latex microspheres*. Advanced Materials, 1999. **11**(11): p. 950-+.
96. Dante, S., et al., *Photoisomerization of polyionic layer-by-layer films containing azobenzene*. Langmuir, 1999. **15**(1): p. 193-201.
97. Lvov, Y., S. Yamada, and T. Kunitake, *Non-linear optical effects in layer-by-layer alternate films of polycations and an azobenzene-containing polyanion*. Thin Solid Films, 1997. **300**(1-2): p. 107-112.

98. Ferreira, M. and M.F. Rubner, *Molecular-Level Processing Of Conjugated Polymers. I. Layer-By-Layer Manipulation Of Conjugated Polyions*. *Macromolecules*, 1995. **28**(21): p. 7107-7114.
99. Saremi, F., et al., *Self-Assembled Alternating Multilayers Built-Up From Diacetylene Bolaamphiphiles And Poly(Allylamine Hydrochloride) - Polymerization Properties, Structure, And Morphology*. *Langmuir*, 1995. **11**(4): p. 1068-1071.
100. Lowack, K. and C.A. Helm, *Polyelectrolyte Monolayers At The Mica/Air Interface - Mechanically Induced Rearrangements And Monolayer Annealing*. *Macromolecules*, 1995. **28**(8): p. 2912-2921.
101. Caruso, F. and H. Mohwald, *Preparation and characterization of ordered nanoparticle and polymer composite multilayers on colloids*. *Langmuir*, 1999. **15**(23): p. 8276-8281.
102. He, J.A., et al., *Electrostatic self-assembly of polydiacetylene nanocrystals: Nonlinear optical properties and chain orientation*. *Journal Of Physical Chemistry B*, 1999. **103**(50): p. 11050-11056.
103. Voigt, A., et al., *Membrane filtration for microencapsulation and microcapsules fabrication by layer-by-layer polyelectrolyte adsorption*. *Industrial & Engineering Chemistry Research*, 1999. **38**(10): p. 4037-4043.
104. Liu, Y.J., A. Rosidian, and R.O. Claus, *Mechanical properties of electrostatically self-assembled Al<sub>2</sub>O<sub>3</sub>-ZrO<sub>2</sub> nanocomposites prepared at room temperature*. *Journal Of Cluster Science*, 1999. **10**(3): p. 421-428.
105. Cheng, L., et al., *Electrochemical growth and characterization of polyoxometalate-containing monolayers and multilayers on alkanethiol monolayers self-assembled on gold electrodes*. *Chemistry Of Materials*, 1999. **11**(6): p. 1465-1475.
106. Liu, Y.J. and R.O. Claus, *Strong enhancement of optical absorbance from ionic self-assembled multilayer thin films of nanocluster Pt and polymer dye*. *Journal Of Applied Physics*, 1999. **85**(1): p. 419-424.

107. Rosidian, A., Y.J. Liu, and R.O. Claus, *Ionic self-assembly of ultrahard ZrO<sub>2</sub>/polymer nanocomposite thin films*. *Advanced Materials*, 1998. **10**(14): p. 1087-+.
108. Yonezawa, T., S.Y. Onoue, and T. Kunitake, *Growth of closely packed layers of gold nanoparticles on an aligned ammonium surface*. *Advanced Materials*, 1998. **10**(5): p. 414-416.
109. Chen, T.Y. and P. Somasundaran, *Preparation of novel core-shell nanocomposite particles by controlled polymer bridging*. *Journal Of The American Ceramic Society*, 1998. **81**(1): p. 140-144.
110. Ingersoll, D., P.J. Kulesza, and L.R. Faulkner, *Polyoxometalate-Based Layered Composite Films On Electrodes - Preparation Through Alternate Immersions In Modification Solutions*. *Journal Of The Electrochemical Society*, 1994. **141**(1): p. 140-147.
111. Shiratori, S.S. and M.F. Rubner, *pH-dependent thickness behavior of sequentially adsorbed layers of weak polyelectrolytes*. *Macromolecules*, 2000. **33**(11): p. 4213-4219.
112. He, J.A., et al., *Bacteriorhodopsin thin film assemblies - Immobilization, properties, and applications*. *Advanced Materials*, 1999. **11**(6): p. 435-+.
113. He, J.A., et al., *Photoelectric properties of oriented bacteriorhodopsin/polycation multilayers by electrostatic layer-by-layer assembly*. *Journal Of Physical Chemistry B*, 1998. **102**(36): p. 7067-7072.
114. He, J.A., et al., *Oriented bacteriorhodopsin/polycation multilayers by electrostatic layer-by-layer assembly*. *Langmuir*, 1998. **14**(7): p. 1674-1679.
115. Brynda, E., et al., *The detection of human beta(2)-microglobulin by grating coupler immunosensor with three dimensional antibody networks*. *Biosensors & Bioelectronics*, 1999. **14**(4): p. 363-368.
116. Caruso, F., et al., *Characterization of polyelectrolyte-protein multilayer films by atomic force microscopy, scanning electron microscopy, and Fourier transform*

- infrared reflection-absorption spectroscopy*. Langmuir, 1998. **14**(16): p. 4559-4565.
117. Kong, W., et al., *Immobilized Bilayer Glucose-Isomerase In Porous Trimethylamine Polystyrene-Based On Molecular Deposition*. Journal Of The Chemical Society-Chemical Communications, 1994(11): p. 1297-1298.
118. Fischer, P., et al., *Polyelectrolytes bearing azobenzenes for the functionalization of multilayers*. Macromolecular Symposia, 1999. **137**: p. 1-24.
119. Dermody, D.L., et al., *Chemically grafted polymeric filters for chemical sensors: Hyperbranched poly(acrylic acid) films incorporating beta-cyclodextrin receptors and amine-functionalized filter layers*. Langmuir, 1999. **15**(3): p. 885-890.
120. Laschewsky, A., et al., *Polyelectrolyte multilayers containing photoreactive groups*. Macromolecular Chemistry And Physics, 1997. **198**(10): p. 3239-3253.
121. Akin, F., et al., *Nanostructure of Fluorocarbon Films Deposited on Polystyrene from C3F5+ Ions*. J Phys Chem B, 2004. **108**: p. 9656-9664.
122. Nelson, B., et al., *Near-Infrared Surface Plasmon Resonance Measurements of Ultrathin Films. 1. Angle Shift and SPR Imaging Experiments*. Anal Chem, 1999. **71**: p. 3928-3934.
123. Hanton, S.D., *Mass Spectrometry of Polymers and Polymer Surfaces*. Chem Rev, 2001. **101**: p. 527-569.
124. Phipps, D.W., et al., *Attenuated Total Reflectance Fourier Transform Infrared (ATR/FT-IR) Spectrometry*, in [http://www.micromemanalytical.com/ATR\\_Ken/ATR.htm](http://www.micromemanalytical.com/ATR_Ken/ATR.htm). 2001.
125. Barr, T.L., *Modern ESCA: The Principles and Practice of X-ray Photoelectron Spectroscopy*. 1994, Boca Raton, FL: CRC Press, Inc.
126. Nefedov, V.I., *X-ray Photoelectron Spectroscopy of Solid Surfaces*. 1988, Utrecht, The Netherlands: VSP.

127. Horiuchi, S., *Fundamentals of High-resolution Transmission Electron Microscopy*. 1994, New York: North-Holland.
128. NUANCE, *HF-2000 User Manual*. 2004  
<<http://www.nuance.northwestern.edu/epic/download/tem-hf2000.html>>.
129. Dykstra, M.J. and L.E. Reuss, *Biological Electron Microscopy: Theory, Techniques, and Troubleshooting*. 2nd ed. 2003, New York: Kluwer Academic/Plenum Publishers.
130. Placinta, G., et al., *Surface properties and the stability of poly(ethylene terephthalate) films treated in plasmas of helium-oxygen mixtures*. *Journal of Applied Polymer Science*, 1997(66): p. 1367-1375.
131. Adanur, S., *Wellington Sears Handbook of Industrial Textiles*. 1995, Lancaster: Technomic Publishing Company.
132. Levasalmi, J. and T.J. McCarthy, *Poly(4-methyl-1-pentene)-Supported Polyelectrolyte Multilayer Films: Preparation and Gas Permeability*. *Macromolecules*, 1997. **30**: p. 1752-1757.